

Higher mass spectra of the fully-charmed and fully-bottom tetraquarks

Feng-Xiao Liu^{1,5}, Ming-Sheng Liu^{2,5}*, Xian-Hui Zhong^{1,5}†, Qiang Zhao^{3,4,5}‡

1) Department of Physics, Hunan Normal University, and Key Laboratory of Low-Dimensional Quantum Structures and Quantum Control of Ministry of Education, Changsha 410081, China

2) College of Science, Tianjin University of Technology, Tianjin 300384, China

3) Institute of High Energy Physics, Chinese Academy of Sciences, Beijing 100049, China

4) University of Chinese Academy of Sciences, Beijing 100049, China and

5) Synergetic Innovation Center for Quantum Effects and Applications (SICQEA), Hunan Normal University, Changsha 410081, China

In this work, we calculate the higher mass spectra for the $2S$ - and $1D$ -wave fully-charmed and fully-bottom tetraquark states in a nonrelativistic potential quark model. The $2S$ -wave fully-charmed/bottom tetraquark states lie in the mass range of $\sim (6.9, 7.1)/(19.7, 19.9)$ GeV, apart from the highest 0^{++} state $T_{(cc\bar{c}\bar{c})0^{++}}(7185)/T_{(bb\bar{b}\bar{b})0^{++}}(19976)$. Most of the $2S$ -wave states highly overlap with the high-lying $1P$ -wave states. The masses for the $1D$ -wave fully-charmed/bottom tetraquark states are predicted to be in the range of $\sim (6.7, 7.2)/(19.5, 20.0)$ GeV. The mass range for the D -wave tetraquark states cover most of the mass range of the P -wave states and the whole mass range of the $2S$ -wave states. The narrow structure $X(6900)$ recently observed at LHCb in the di- J/ψ invariant mass spectrum may be caused by the $1P$ -, or $2S$ -, or $1D$ -wave $T_{(cc\bar{c}\bar{c})}$ states. The vague structure $X(7200)$ may be caused by the highest $2S$ -wave state $T_{(cc\bar{c}\bar{c})0^{++}}(7185)$, two low-lying $3S$ -wave states $T_{(cc\bar{c}\bar{c})0^{++}}(7240)$ and $T_{(cc\bar{c}\bar{c})2^{++}}(7248)$, and/or the high-lying $1D$ -wave states with masses around 7.2 GeV and $J^{PC} = 0^{++}, 1^{++}, 2^{++}, 3^{++},$ or 4^{++} . While it is apparent that the potential quark model calculations predict more states than the structures observed in the di- J/ψ invariant mass spectrum, our calculations will help further understanding of the properties of these fully-heavy tetraquark states in their strong and magnetic interactions with open channels based on explicit quark model wave functions.

PACS numbers:

I. INTRODUCTION

Recently, the LHCb Collaboration reported their results on the observations of full-charmed tetraquark $cc\bar{c}\bar{c}$ ($T_{(cc\bar{c}\bar{c})}$) states [1]. Using the full Run1 and Run2 LHCb data of 9 fb^{-1} , the di- J/ψ invariant mass spectrum was studied at $p_T > 5.2 \text{ GeV}/c$. A broad structure above threshold ranging from 6.2 to 6.8 GeV [denoted by $X(6200 - 6800)$] and a narrower structure at about 6.9 GeV [denoted by $X(6900)$] are observed with more than 5σ of significance level. There is also a vague structure around 7.2 GeV [denoted by $X(7200)$] to be confirmed. These clear structures may be evidences for genuine tetraquark $T_{(cc\bar{c}\bar{c})}$ states arising from the quark-gluon interactions in QCD rather than loosely bound hadronic molecules [2, 3], since the light mesons cannot be exchanged between two heavy mesons.

Before the LHCb observations, the $T_{(cc\bar{c}\bar{c})}$ spectrum has been widely studied in the literature [4–31]. With the observations at LHCb, the fully-heavy tetraquark system has again attracted a lot attention from the community. Theoretical studies of various properties of such systems can be found in the literature, such as calculations of the mass spectrum [32–55], production mechanisms [56–62], strong decays [63, 64], and analyses of the measured di- J/ψ invariant mass spectrum [65–71] based on different scenarios.

So far, the theoretical interpretations of the LHCb observations are various. For the broad structure $X(6200 - 6800)$,

many analyses based on the mass location [23–46] indicate that it could be a good candidate of the ground $T_{(cc\bar{c}\bar{c})}$ states with $J^{PC} = 0^{++}$ and 2^{++} . In contrast, some other models have predicted relatively lower masses than 6200 MeV for the 0^{++} and 2^{++} ground states [11–16, 47–50]. There, the $X(6200 - 6800)$ may be assigned to some excited states.

For the narrow structure $X(6900)$, theoretical interpretations are far from convergent. In the present literature, $X(6900)$ is suggested to be a candidate of the $2S$ -wave (i.e., the first radial excitation) state by several quark model calculations, which include the nonrelativistic potential models [39, 40, 51], relativistic quark model [36], extended relativized quark model [46], dynamical diquark model [52], and the string-junction picture [41]. However, it is also assigned as a candidate of some higher $T_{(cc\bar{c}\bar{c})}$ excitations by other models. Its assignments include as a $3S$ -wave state [34, 48–50], $1D$ -wave state [29, 36], $1P$ -wave state [26, 29, 32, 51], and a $2P$ -wave state [50].

Attention is also paid to the vague structure $X(7200)$ in the di- J/ψ invariant mass spectrum [1]. In the spectrum studies, it is assigned as higher excitation states, such as the second radial ($3S$) excitations [36, 40], some $2P$ and/or $2D$ excitations [52].

Apart from the interpretations which treat these signals as genuine tetraquark states, there are also other explanations proposed in the literature. For instance, Refs. [67–69] describe the structures appearing in the di- J/ψ invariant mass spectrum by coupled-channel effects of double-charmonium rescatterings via an effective potential. In Ref. [70], it is proposed that the Pomeron exchange between two vector charmonium states can provide strong near-threshold couplings and then dynamically generate pole structures above the two vector charmonium thresholds. Other solutions include treat-

*E-mail: liumingsheng0001@126.com

†E-mail: zhongxh@hunnu.edu.cn

‡E-mail: zhaoq@ihep.ac.cn

ing the narrow $X(6900)$ as a light Higgs-like boson [73], and $X(6900)$ and $X(7200)$ as gluonic tetracharm states [72], or $\Xi_{cc}\Xi_{cc}$ molecules [74].

In our previous works [28, 32], we have systematically studied the mass spectra of the $1S$ and $1P$ -wave $T_{(cc\bar{c}\bar{c})}$ states within a nonrelativistic potential quark model (NRPQM). Their masses are predicted to be within the ranges of $\sim (6445, 6550)$ MeV and $\sim (6600, 7000)$ MeV, respectively. Our results show that the broad structure $X(6200 - 6800)$ is consistent with the $1S$ -wave states around 6.5 GeV, which is similar to the conclusions from Refs. [23–46]. It should be mentioned that some low-lying $1P$ -wave states with a mass around 6.7 GeV may contribute to $X(6200 - 6800)$ as well. Furthermore, it is found that the narrow structure $X(6900)$ may correspond to some $1P$ -wave states around 6.9 GeV with $J^{PC} = 0^{-+}, 1^{-+}, 2^{-+}$. Such a possibility was also discussed by the recent potential quark model calculations [29, 51] and the previous QCD sum rule predictions [26]. Actually, since quite a lot of states are predicted by the tetraquark picture, we will see later that some other possibilities, such as $2S$ -, and $1D$ -wave states, cannot be eliminated. The vague structure $X(7200)$ lies about 200 MeV above the high-lying $1P$ -wave states according to our potential quark model predictions [32]. Given that higher excited states should exist in the quark model, the structure of $X(7200)$ may be an indications of some higher excitations. This is also one of our motivations to investigate the higher $T_{(cc\bar{c}\bar{c})}$ mass spectrum in order to understand the nature of $X(7200)$.

In this work, we continue to study the mass spectra for the higher $2S$ -, $3S$ -, and $1D$ -wave fully-heavy tetraquark states, i.e. $T_{(QQ\bar{Q}\bar{Q})}$ ($Q = c, b$). The main purposes are: (i) to investigate the possibility of assigning $X(6900)$ as the $2S$ - and/or $1D$ -wave states in the mass spectrum within a consistent framework; (ii) to know whether or not the $X(7200)$ structure can be associated with the high $2S$ -, $3S$ -, and/or $1D$ -wave $T_{(cc\bar{c}\bar{c})}$ excitations; (iii) to give relatively complete $T_{(QQ\bar{Q}\bar{Q})}$ spectra up to the second orbital excitation. It should be mentioned that many studies of the spectrum of the radial (S -wave) excitations have been carried out [36, 39, 40, 46, 51, 52]. However, because of the complexity of dealing with the four-body system, the study of higher excited states progresses rather slowly. So far, the theoretical predictions on some special $1D$ -wave states are based on either the diquark-antidiquark picture, or spin-flavor symmetries as a scheme for parametrization [15, 29, 36, 52]. For the tetraquark orbital excitations, the spin-orbital and tensor couplings will contribute to the Hamiltonian which will lead to configuration mixings in the wave functions. Thus, the calculation of an orbital excitation tetraquark system turns out to be more challenging than that for a radial excitation.

The NRPQM adopted in the present work is based on the Hamiltonian from the Cornell model [75], which contains a linear confinement potential, a Coulomb-like potential, spin-spin interactions, spin-orbital interactions, and tensor potentials. With the NRPQM, we have studied both the $1S$ - and $1P$ -wave fully-heavy and fully-strange tetraquark states [28, 32, 76] with a Gaussian expansion method [77, 78]. In our calculations, we deal with the fully-heavy tetraquark

systems without the diquark-antidiquark approximation. With the same parameter set as that for our calculations of the $1S$ - and $1P$ -wave $T_{(QQ\bar{Q}\bar{Q})}$ ($Q = c, b$) states in Refs. [28, 32], we obtain self-consistent predictions of the $T_{(QQ\bar{Q}\bar{Q})}$ mass spectrum for 12 $2S/3S$ -wave radial excitations, and 80 $1D$ -wave orbital excitations.

The paper is organized as follows: a brief introduction to the methodology for the tetraquark spectrum is given in Sec. II. In Sec. III, the numerical results and discussions are presented. A short summary is given in Sec. IV.

II. METHODOLOGY

A. Hamiltonian

We adopt a NRPQM to calculate the masses of the tetraquark states. In this model, the Hamiltonian is given by

$$H = \left(\sum_{i=1}^4 m_i + T_i \right) - T_G + \sum_{i < j} V_{ij}(r_{ij}), \quad (1)$$

where m_i and T_i stand for the constituent quark mass and kinetic energy of the i th quark, respectively; T_G stands for the center-of-mass (c.m.) kinetic energy of the tetraquark system; $r_{ij} \equiv |\mathbf{r}_i - \mathbf{r}_j|$ is the distance between the i th and j th quarks; and $V_{ij}(r_{ij})$ stands for the effective potential between them. In this work the $V_{ij}(r_{ij})$ adopts a widely used form [75, 76, 79–90]:

$$V_{ij}(r_{ij}) = V_{ij}^{conf}(r_{ij}) + V_{ij}^{sd}(r_{ij}), \quad (2)$$

where the confinement potential adopts the standard form of the Cornell potential [75], which includes the spin-independent linear confinement potential $V_{ij}^{Lin}(r_{ij}) \propto r_{ij}$ and Coulomb-like potential $V_{ij}^{Coul}(r_{ij}) \propto 1/r_{ij}$:

$$V_{ij}^{conf}(r_{ij}) = -\frac{3}{16}(\lambda_i \cdot \lambda_j) \left(b_{ij} r_{ij} - \frac{4}{3} \frac{\alpha_{ij}}{r_{ij}} + C_0 \right). \quad (3)$$

The constant C_0 stands for the zero point energy. While the spin-dependent potential $V_{ij}^{sd}(r_{ij})$ is the sum of the spin-spin contact hyperfine potential V_{ij}^{SS} , the spin-orbit potential V_{ij}^{SO} , and the tensor term V_{ij}^T :

$$V_{ij}^{sd}(r_{ij}) = V_{ij}^{SS} + V_{ij}^T + V_{ij}^{LS}, \quad (4)$$

with

$$V_{ij}^{SS} = -\frac{\alpha_{ij}}{4}(\lambda_i \cdot \lambda_j) \left\{ \frac{\pi}{2} \cdot \frac{\sigma_{ij}^3 e^{-\sigma_{ij}^2 r_{ij}^2}}{\pi^{3/2}} \cdot \frac{16}{3m_i m_j} (\mathbf{S}_i \cdot \mathbf{S}_j) \right\}, \quad (5)$$

$$V_{ij}^{LS} = -\frac{\alpha_{ij}}{16} \frac{\lambda_i \cdot \lambda_j}{r_{ij}^3} \left(\frac{1}{m_i^2} + \frac{1}{m_j^2} + \frac{4}{m_i m_j} \right) \left\{ \mathbf{L}_{ij} \cdot (\mathbf{S}_i + \mathbf{S}_j) \right\} - \frac{\alpha_{ij}}{16} \frac{\lambda_i \cdot \lambda_j}{r_{ij}^3} \left(\frac{1}{m_i^2} - \frac{1}{m_j^2} \right) \left\{ \mathbf{L}_{ij} \cdot (\mathbf{S}_i - \mathbf{S}_j) \right\}, \quad (6)$$

$$V_{ij}^T = -\frac{\alpha_{ij}}{4}(\lambda_i \cdot \lambda_j) \cdot \frac{1}{m_i m_j r_{ij}^3} \left\{ \frac{3(\mathbf{S}_i \cdot \mathbf{r}_{ij})(\mathbf{S}_j \cdot \mathbf{r}_{ij})}{r_{ij}^2} - \mathbf{S}_i \cdot \mathbf{S}_j \right\}. \quad (7)$$

In the above equations, \mathbf{S}_i stands for the spin of the i th quark, and \mathbf{L}_{ij} stands for the relative orbital angular momentum between the i th and j th quarks. If the interaction occurs between two quarks or antiquarks, the $\lambda_i \cdot \lambda_j$ operator is defined as $\lambda_i \cdot \lambda_j \equiv \sum_{a=1}^8 \lambda_i^a \lambda_j^a$, while if the interaction occurs between a quark and an antiquark, the $\lambda_i \cdot \lambda_j$ operator is defined as $\lambda_i \cdot \lambda_j \equiv \sum_{a=1}^8 -\lambda_i^a \lambda_j^{a*}$, where λ^{a*} is the complex conjugate of the Gell-Mann matrix λ^a . The parameters b_{ij} and α_{ij} denote the strength of the confinement and strong coupling of the one-gluon-exchange potential, respectively. The quark model parameter sets $\{m_c, \alpha_{cc}, \sigma_{cc}, b_{cc}\}$ and $\{m_b, \alpha_{bb}, \sigma_{bb}, b_{bb}\}$ are taken the same as those in Refs. [28, 32, 86], they are determined by fitting the charmonium and bottomonium spectra. The quark model parameters adopted in this work are collected in the Table I.

TABLE I: Quark model parameters used in this work.

m_c/m_b (GeV)	1.483/4.852
α_{cc}/α_{bb}	0.5461/0.4311
σ_{cc}/σ_{bb} (GeV)	1.1384/2.3200
b_{cc}/b_{bb} (GeV ²)	0.1425/0.1425

B. Tetraquark configurations

The wave function for a $qq\bar{q}\bar{q}$ system can be constructed as a product of the flavor, color, and spatial configurations.

In the color space, there are two color-singlet bases $|\mathbb{6}\bar{\mathbb{6}}\rangle_c$ and $|\mathbb{3}\bar{\mathbb{3}}\rangle_c$, their wave functions are given by

$$|\mathbb{6}\bar{\mathbb{6}}\rangle_c = \frac{1}{2\sqrt{6}} \left[(rb + br)(\bar{b}\bar{r} + \bar{r}\bar{b}) + (gr + rg)(\bar{g}\bar{r} + \bar{r}\bar{g}) + (gb + bg)(\bar{b}\bar{g} + \bar{g}\bar{b}) + 2(rr)(\bar{r}\bar{r}) + 2(gg)(\bar{g}\bar{g}) + 2(bb)(\bar{b}\bar{b}) \right], \quad (8)$$

$$|\mathbb{3}\bar{\mathbb{3}}\rangle_c = \frac{1}{2\sqrt{3}} \left[(br - rb)(\bar{b}\bar{r} - \bar{r}\bar{b}) - (rg - gr)(\bar{g}\bar{r} - \bar{r}\bar{g}) + (bg - gb)(\bar{b}\bar{g} - \bar{g}\bar{b}) \right]. \quad (9)$$

In the spin space, there are six spin bases, which are denoted by $\chi_{S_2 S_4}^{S_{12} S_{34}}$. Where S_{12} stands for the spin quantum number for the diquark ($q_1 q_2$) (or antidiquark ($\bar{q}_1 \bar{q}_2$)), while S_{34} stands for the spin quantum number for the antidiquark ($\bar{q}_3 \bar{q}_4$) (or diquark ($q_3 q_4$)). S is the total spin quantum number of the tetraquark $qq\bar{q}\bar{q}$ system, while S_z stands for the third component of the total spin \mathbf{S} . The spin wave functions $\chi_{S_2 S_4}^{S_{12} S_{34}}$ with

a determined S_z can be explicitly expressed as follows:

$$\chi_{00}^{00} = \frac{1}{2}(\uparrow\downarrow\uparrow\downarrow - \uparrow\downarrow\downarrow\uparrow - \downarrow\uparrow\uparrow\downarrow + \downarrow\uparrow\downarrow\uparrow), \quad (10)$$

$$\chi_{00}^{11} = \sqrt{\frac{1}{12}}(2\uparrow\uparrow\downarrow\downarrow - \uparrow\downarrow\uparrow\downarrow - \uparrow\downarrow\downarrow\uparrow - \downarrow\uparrow\uparrow\downarrow - \downarrow\uparrow\downarrow\uparrow + 2\downarrow\downarrow\uparrow\uparrow), \quad (11)$$

$$\chi_{11}^{01} = \sqrt{\frac{1}{2}}(\uparrow\downarrow\uparrow\uparrow - \downarrow\uparrow\uparrow\uparrow), \quad (12)$$

$$\chi_{11}^{10} = \sqrt{\frac{1}{2}}(\uparrow\uparrow\uparrow\downarrow - \uparrow\uparrow\downarrow\uparrow), \quad (13)$$

$$\chi_{11}^{11} = \frac{1}{2}(\uparrow\uparrow\uparrow\downarrow + \uparrow\uparrow\downarrow\uparrow - \uparrow\downarrow\uparrow\uparrow - \downarrow\uparrow\uparrow\uparrow), \quad (14)$$

$$\chi_{22}^{11} = \uparrow\uparrow\uparrow\uparrow. \quad (15)$$

In the spatial space, we define the relative Jacobi coordinates with the single-partial coordinates \mathbf{r}_i ($i = 1, 2, 3, 4$):

$$\xi_1 \equiv \mathbf{r}_1 - \mathbf{r}_2, \quad (16)$$

$$\xi_2 \equiv \mathbf{r}_3 - \mathbf{r}_4, \quad (17)$$

$$\xi_3 \equiv \frac{m_1 \mathbf{r}_1 + m_2 \mathbf{r}_2}{m_1 + m_2} - \frac{m_3 \mathbf{r}_3 + m_4 \mathbf{r}_4}{m_3 + m_4}, \quad (18)$$

$$\mathbf{R} \equiv \frac{m_1 \mathbf{r}_1 + m_2 \mathbf{r}_2 + m_3 \mathbf{r}_3 + m_4 \mathbf{r}_4}{m_1 + m_2 + m_3 + m_4}. \quad (19)$$

Note that ξ_1 and ξ_2 stand for the relative Jacobi coordinates between two quarks q_1 and q_2 (or antiquarks \bar{q}_1 and \bar{q}_2), and two antiquarks \bar{q}_3 and \bar{q}_4 (or quarks q_3 and q_4), respectively. While ξ_3 stands for the relative Jacobi coordinate between diquark qq and antidiquark $\bar{q}\bar{q}$.

The spatial bases describing the intrinsic motion of the system with principal quantum number N and orbital angular momentum quantum numbers LM , ψ_{NLM} , can be expressed as the linear combination $\psi_{\alpha_1}(\xi_1)\psi_{\alpha_2}(\xi_2)\psi_{\alpha_3}(\xi_3)$:

$$\psi_{NLM} = \sum_{\alpha_1, \alpha_2, \alpha_3} C_{\alpha_1, \alpha_2, \alpha_3} [\psi_{\alpha_1}(\xi_1)\psi_{\alpha_2}(\xi_2)\psi_{\alpha_3}(\xi_3)]_{NLM}, \quad (20)$$

where $C_{\alpha_1, \alpha_2, \alpha_3}$ are the combination coefficients. The functions $\psi_{\alpha_i}(\xi_i)$ ($i = 1, 2, 3$) stand for the relative-motion wave functions for the relative Jacobi coordinates ξ_i . In the quantum number set $\alpha_i \equiv \{n_{\xi_i}, l_{\xi_i}, m_{\xi_i}\}$, n_{ξ_i} is the principal quantum number, l_{ξ_i} is the angular momentum, and m_{ξ_i} is its third component projection. For example, for the $1D$ -wave states six

spatial bases with $M = 0$ can be explicitly expressed as

$$|\psi_{020}^{\xi_1}\rangle = \psi_{020}(\xi_1)\psi_{000}(\xi_2)\psi_{000}(\xi_3), \quad (21)$$

$$|\psi_{020}^{\xi_2}\rangle = \psi_{000}(\xi_1)\psi_{020}(\xi_2)\psi_{000}(\xi_3), \quad (22)$$

$$|\psi_{020}^{\xi_3}\rangle = \psi_{000}(\xi_1)\psi_{000}(\xi_2)\psi_{020}(\xi_3), \quad (23)$$

$$\begin{aligned} |\psi_{020}^{\xi_1\xi_2}\rangle &= +\frac{1}{\sqrt{6}}\psi_{011}(\xi_1)\psi_{01-1}(\xi_2)\psi_{000}(\xi_3) \\ &+ \sqrt{\frac{2}{3}}\psi_{010}(\xi_1)\psi_{010}(\xi_2)\psi_{000}(\xi_3) \\ &+ \frac{1}{\sqrt{6}}\psi_{01-1}(\xi_1)\psi_{011}(\xi_2)\psi_{000}(\xi_3), \end{aligned} \quad (24)$$

$$\begin{aligned} |\psi_{010}^{\xi_1\xi_2}\rangle &= +\frac{1}{\sqrt{2}}\psi_{011}(\xi_1)\psi_{01-1}(\xi_2)\psi_{000}(\xi_3) \\ &- \frac{1}{\sqrt{2}}\psi_{01-1}(\xi_1)\psi_{011}(\xi_2)\psi_{000}(\xi_3), \end{aligned} \quad (25)$$

$$\begin{aligned} |\psi_{000}^{\xi_1\xi_2}\rangle &= +\frac{1}{\sqrt{3}}\psi_{011}(\xi_1)\psi_{01-1}(\xi_2)\psi_{000}(\xi_3) \\ &- \sqrt{\frac{1}{3}}\psi_{010}(\xi_1)\psi_{010}(\xi_2)\psi_{000}(\xi_3) \\ &+ \frac{1}{\sqrt{3}}\psi_{01-1}(\xi_1)\psi_{011}(\xi_2)\psi_{000}(\xi_3). \end{aligned} \quad (26)$$

For the $2S$ -wave states, the three spatial bases are explicitly expressed as

$$|\psi_{100}^{\xi_1}\rangle = \psi_{100}(\xi_1)\psi_{000}(\xi_2)\psi_{000}(\xi_3), \quad (27)$$

$$|\psi_{100}^{\xi_2}\rangle = \psi_{000}(\xi_1)\psi_{100}(\xi_2)\psi_{000}(\xi_3), \quad (28)$$

$$|\psi_{100}^{\xi_3}\rangle = \psi_{000}(\xi_1)\psi_{000}(\xi_2)\psi_{100}(\xi_3). \quad (29)$$

The superscript ξ_i ($i = 1, 2, 3$) of the bases stands for an excitation (i.e., ξ_i -mode excitation) appearing within the intrinsic wave function $\psi_{\alpha_i}(\xi_i)$, while the superscript $\xi_i\xi_j$ stands for an excitation ($\xi_i\xi_j$ -mode excitation) appearing within both the $\psi_{\alpha_i}(\xi_i)$ and $\psi_{\alpha_j}(\xi_j)$ at the same time.

Taking into account the Pauli principle and color confinement for the four-quark system $qq\bar{q}\bar{q}$, one has 12 configurations for the $2S$ -wave radial excitations, and 80 configurations for the $1D$ -wave orbital excitations. The higher radially excited configurations corresponding to the same excited modes of these $2S$ -wave configurations are also easily obtained. The spin-parity quantum numbers, notations, and total wave functions for these $2S/3S$ - and $1D$ -wave configurations are presented in Tables II, III and IV.

C. Numerical method

To work out the matrix elements in the coordinate space, we follow the same method adopted in our previous works [28, 32, 76]. As we know, the relative-motion wave functions $\psi_{\alpha_i}(\xi_i)$ can be expressed as

$$\psi_{\alpha_i}(\xi_i) = R_{n_{\xi_i}l_{\xi_i}}(\xi_i)Y_{l_{\xi_i}m_{\xi_i}}(\hat{\xi}_i), \quad (30)$$

where $Y_{l_{\xi_i}m_{\xi_i}}(\hat{\xi}_i)$ are the standard spherical harmonic functions. The unknown radial parts, $R_{n_{\xi_i}l_{\xi_i}}(\xi_i)$, are expanded with a series of Gaussian basis functions [32, 88]:

$$R_{n_{\xi_i}l_{\xi_i}}(\xi) = \sum_{\ell=1}^n C_{\xi\ell} \phi_{n_{\xi_i}l_{\xi_i}}(d_{\xi_i\ell}, \xi_i), \quad (31)$$

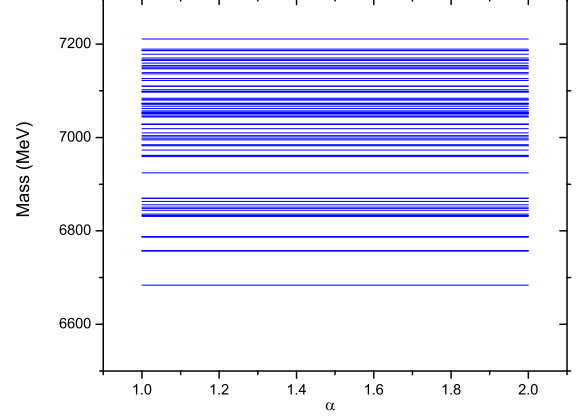


FIG. 1: Predicted masses of 80 $1D$ -wave $T_{(ccc\bar{c})}$ configurations as functions of the scaling factor α .

with

$$\phi_{n_{\xi_i}l_{\xi_i}}(d_{\xi_i\ell}, \xi_i) = \left(\frac{1}{d_{\xi_i\ell}}\right)^{\frac{3}{2}} \left[\frac{2^{\ell_{\xi_i}+2}}{(2\ell_{\xi_i}+1)!!\sqrt{\pi}}\right]^{\frac{1}{2}} \left(\frac{\xi_i}{d_{\xi_i\ell}}\right)^{l_{\xi_i}} e^{-\frac{1}{2}\left(\frac{\xi_i}{d_{\xi_i\ell}}\right)^2}. \quad (32)$$

It should be pointed out that if there are no radial excitations, the expansion method with Gaussian basis functions are just the same as the expansion method with harmonic oscillator wave functions. The parameter $d_{\xi_i\ell}$ in Eq. (31) can be related to the harmonic oscillator frequency $\omega_{\xi_i\ell}$ with $1/d_{\xi_i\ell}^2 = \mu_{\xi_i}\omega_{\xi_i\ell}$. For a tetraquark state $T_{(qq\bar{q}\bar{q})}$ containing fully-equal mass quarks, if we ensure that the spatial wave function with Jacobi coordinates can transform into the single particle coordinates, the harmonic oscillator frequencies $\omega_{\xi_i\ell}$ ($i = 1, 2, 3$) can be related to the harmonic oscillator stiffness factor K_ℓ with $\omega_{\xi_1\ell} = \sqrt{2K_\ell/\mu_{\xi_1}}$, $\omega_{\xi_2\ell} = \sqrt{2K_\ell/\mu_{\xi_2}}$, and $\omega_{\xi_3\ell} = \sqrt{4K_\ell/\mu_{\xi_3}}$. Taking the reduced masses $\mu_{\xi_1} = \mu_{\xi_2} = m_q/2$, $\mu_{\xi_3} = m_q$ for $T_{(qq\bar{q}\bar{q})}$, one has $\omega_{\xi_1\ell} = \omega_{\xi_2\ell} = \omega_{\xi_3\ell} = \omega_\ell$ and $d_{\xi_i\ell} = (m_q/\mu_{\xi_i})^{1/2}d_\ell$ with $d_\ell = (4m_qK_\ell)^{-1/4}$.

Then, the expansion of $\prod_{i=1}^3 R_{n_{\xi_i}l_{\xi_i}}(\xi_i)$ can be simplified as

$$\prod_{i=1}^3 R_{n_{\xi_i}l_{\xi_i}}(\xi_i) = \sum_{\ell}^n C_\ell \prod_{i=1}^3 \phi_{n_{\xi_i}l_{\xi_i}}(d_{\xi_i\ell}, \xi_i). \quad (33)$$

Following the method of Refs. [77, 78], we let the d_ℓ parameters form a geometric progression

$$d_\ell = d_1 a^{\ell-1} \quad (\ell = 1, \dots, n), \quad (34)$$

where n is the number of Gaussian basis functions, and a is the ratio coefficient. There are three parameters $\{d_1, d_n, n\}$ to be determined through the variation method. It is found that with the parameter sets, $\{0.068 \text{ fm}, 2.711 \text{ fm}, 15\}$ and $\{0.050 \text{ fm}, 2.016 \text{ fm}, 15\}$, for the $cc\bar{c}\bar{c}$ and $bb\bar{b}\bar{b}$ systems, respectively, we can obtain stable solutions. The numerical results should be independent of the parameter d_1 . To confirm this point, as done in the literature [91–93] we scale the parameter d_1 of the

basis functions as $d_1 \rightarrow \alpha d_1$. The mass of a $T_{(QQ\bar{Q}\bar{Q})}$ ($Q = c, b$) state should be stable at a resonance energy insensitive to the scaling parameter α . As an example, we plot the masses of 80 1D-wave $T_{(cc\bar{c}\bar{c})}$ configurations as a function of the scaling factor α in Fig. 1. It is found that the numerical results are nearly independent of the scaling factor α . The stabilization of other states predicted in this work has also been examined by the same method. With the mass matrix elements ready for every configuration, the mass of the tetraquark configuration and its spacial wave function can be determined by solving a generalized eigenvalue problem. The details can be found in our previous works [28, 88]. The physical states can be obtained by diagonalizing the mass matrix of different configurations with the same J^{PC} numbers.

Finally, we give some discussions of the numerical method adopted in present work. Usually the trial spatial wave functions are expanded by a series of Gaussian functions. To keep the completeness of the Gaussian basis set, and to precisely treat an N -body system, one can involve several different sets of Jacobi coordinates as those done in Refs. [77, 78, 91–94], or adopt a single set of Jacobi coordinates $X = (\xi_1, \xi_2, \dots, \xi_{N-1})$ with non diagonal Gaussians e^{-XAX^T} as those done in Refs. [95–98], where A is a symmetric matrix. In our work, we deal with the $cc\bar{c}\bar{c}$ and $bb\bar{b}\bar{b}$ systems which are composed of equal mass constituent quarks and antiquarks. With equal quark masses, a non diagonal term with $\exp\{\dots + \beta\xi_i \cdot \xi_j \dots\}$ ($i \neq j$) implies another one with $\exp\{\dots - \beta\xi_i \cdot \xi_j \dots\}$, so that the contribution of first order in β is eliminated. Thus, the equal mass symmetry can let us select a single set of Jacobi coordinates with a diagonal Gaussian basis set as an approximation in our study. In this work, the advantage of adopting a single Jacobi coordinates is that: (i) all the configurations are orthogonal compact multiquark configurations; (ii) its basis functions are significantly less than those of several different sets of Jacobi coordinates. However, with several different sets of Jacobi coordinates, even the continuum states corresponding to the hadron-hadron scattering solutions come out as discrete states, therefore, one needs adopt a method, such as the real-scaling method, to distinguish the genuine resonances from the discretized scattering states [92]. It should be mentioned that if one deals with a multiquark system composed of mass-different quarks, a single set of Jacobi coordinates with a diagonal Gaussian basis set may be not a good approximation.

III. RESULTS AND DISCUSSIONS

Our predicted mass spectra for the 2S/3S-wave $T_{(cc\bar{c}\bar{c})}$ and $T_{(bb\bar{b}\bar{b})}$ states are presented in Tables V and VI, respectively. The predictions for the 1D-wave $T_{(cc\bar{c}\bar{c})}$ states are given in Tables VII and VIII, and the predictions for the 1D-wave $T_{(bb\bar{b}\bar{b})}$ states are given in Tables IX and X. From these tables the components of different configurations for a physical state can be seen. To see the contributions from each part of the Hamiltonian to the mass of different configurations, we also present our results in Tables XI–XVI.

We find that both the kinetic energy term $\langle T \rangle$ and the lin-

ear confinement potential term $\langle V^{Lin} \rangle$ contribute large positive values to the masses, while the Coulomb type potential $\langle V^{Coul} \rangle$ has a large cancellation with these two terms. The spin-spin interaction term $\langle V^{SS} \rangle$, the tensor potential term $\langle V^T \rangle$, and/or the spin-orbit interaction term $\langle V^{LS} \rangle$ have also sizeable contributions to some configurations. It suggests that a reliable calculation should include both the spin-independent and spin-dependent potentials in the calculations for the tetraquarks. For illustration, our predicted $T_{(cc\bar{c}\bar{c})}$ and $T_{(bb\bar{b}\bar{b})}$ spectra are plotted in Figs. 2 and 3, respectively.

A. 2S and 3S states

In the radially excited (2S-, 3S-wave, etc.) states, apart from the 1S ground states with the same quantum numbers, i.e., $J^{PC} = 0^{++}, 1^{+-}, 2^{++}$, some states with additional quantum numbers, i.e., $J^{PC} = 0^{+-}, 1^{++}, 2^{+-}$, can also be accessed. It should be mentioned that by fully expanding $\prod_{i=1}^3 R_{n_{\xi_i} l_{\xi_i}}(\xi_i)$ with the GEM, one cannot distinguish the ξ_1 and ξ_2 excitation modes which are defined for the 2S/3S configurations listed in Table II. As a consequence, it is not possible to numerically work out the masses for the configurations with $J^{PC} = 0^{+-}, 1^{++}, 2^{+-}$. To overcome this problem, following the method adopted in Ref. [76] we only expand the spatial wave functions containing the radial excitations with series of Gaussian basis functions, while for those spatial wave functions containing no excitations we adopt the single Gaussian function as an approximation.

There often exist configuration mixings among the states with the same J^{PC} quantum numbers, which can be seen from the results listed in Tables V and VI. For example, there is an obvious mixing between the two 0^{+-} states $2^1 S_{0^{+-}(\bar{6}\bar{6})_c(\xi_1, \xi_2)}$ and $2^1 S_{0^{+-}(\bar{3}\bar{3})_c(\xi_1, \xi_2)}$ in the $T_{(cc\bar{c}\bar{c})}$ family due to the sizeable off-diagonal elements contributed by the spin-spin interaction together with the nearly equal masses for these two 0^{+-} configurations. In contrast, the mixing between the two 0^{+-} $T_{(bb\bar{b}\bar{b})}$ states due to the spin-spin interaction is strongly suppressed by the heavy bottom quark mass. The sizeable mixing between the two 2^{++} states $2^5 S_{2^{++}(\bar{3}\bar{3})_c(\xi_1, \xi_2)}$ and $2^5 S_{2^{++}(\bar{3}\bar{3})_c(\xi_3)}$ is mainly caused by the Coulomb type potential. The Coulomb type potential together with the linear confinement potential will cause a sizeable mixing between the two 1^{+-} configurations $2^3 S_{1^{+-}(\bar{3}\bar{3})_c(\xi_1, \xi_2)}$ and $2^3 S_{1^{+-}(\bar{3}\bar{3})_c(\xi_3)}$.

In the configurations with the same J^{PC} , the Coulomb type potentials $\langle V^{Coul} \rangle$ for the $|\bar{3}\bar{3}\rangle_c$ structure are always more attractive than that for the $|\bar{6}\bar{6}\rangle_c$ structure. However, in some cases a $|\bar{3}\bar{3}\rangle_c$ configuration may have a larger mass than the $|\bar{6}\bar{6}\rangle_c$ configuration due to the larger contributions from the linear confinement potential term $\langle V^{Lin} \rangle$ and kinetic energy term $\langle T \rangle$. For example, for the $T_{(cc\bar{c}\bar{c})}$ sector the $|\bar{6}\bar{6}\rangle_c$ configuration $2^1 S_{0^{++}(\bar{6}\bar{6})_c(\xi_1, \xi_2)}$ has a mass of 6954 MeV, which is about 46 MeV smaller than that for the $|\bar{3}\bar{3}\rangle_c$ configuration $2^1 S_{0^{++}(\bar{3}\bar{3})_c(\xi_1, \xi_2)}$ of which the mass is 7000 MeV. It is seen that the contributions $\langle T \rangle = 725$ MeV and $\langle V^{Lin} \rangle = 883$ MeV for $2^1 S_{0^{++}(\bar{6}\bar{6})_c(\xi_1, \xi_2)}$ are smaller than $\langle T \rangle = 774$ MeV and $\langle V^{Lin} \rangle = 919$ MeV for $2^1 S_{0^{++}(\bar{3}\bar{3})_c(\xi_1, \xi_2)}$, while $\langle V^{Coul} \rangle = -622$ MeV for

$2^1S_{0^{++}(\bar{3}\bar{3})_c(\xi_1, \xi_2)}$ is more attractive than $\langle V^{Coul} \rangle = -598$ MeV for $2^1S_{0^{++}(\bar{6}\bar{6})_c(\xi_1, \xi_2)}$. It should be mentioned that in the configurations with the same J^{PC} , the lowest mass state is the radial excitation between the diquark (qq) and antiquark ($\bar{q}\bar{q}$) (i.e. the ξ_3 -mode excitation) with the $|\bar{3}\bar{3}\rangle_c$ structure due to the most attractive Coulomb type potential term $\langle V^{Coul} \rangle$ together with the smallest linear confinement potential term $\langle V^{Lin} \rangle$.

Including configuration mixing effects, the physical masses for the $2S$ $T_{(cc\bar{c}\bar{c})}$ are predicted to be in the range of $\sim (6900, 7000)$ MeV, except for one 0^{++} state $T_{(cc\bar{c}\bar{c})0^{++}}(7185)$ which has a mass of $M = 7185$ MeV. The masses for the $3S$ $T_{(cc\bar{c}\bar{c})}$ are predicted to be in the range of $\sim (7200, 7400)$ MeV, except for the highest 0^{++} state $T_{(cc\bar{c}\bar{c})0^{++}}(7720)$. The masses for most of the $2S$ $T_{(bb\bar{b}\bar{b})}$ are predicted to be in the range of $\sim (19720, 19840)$ MeV, except for the highest 0^{++} state $T_{(bb\bar{b}\bar{b})0^{++}}(19976)$. Similarly, the masses for most of the $3S$ $T_{(bb\bar{b}\bar{b})}$ are predicted to be in the range of $\sim (19980, 20130)$ MeV, except for the highest 0^{++} state $T_{(bb\bar{b}\bar{b})0^{++}}(20405)$. The gap between the lowest $2S$ $T_{(cc\bar{c}\bar{c})}$ state and the highest $1S$ $T_{(cc\bar{c}\bar{c})}$ state is about 358 MeV, which is very close to the value ~ 368 MeV for the $T_{(bb\bar{b}\bar{b})}$ sector. Our predictions for the $2S$ $T_{(cc\bar{c}\bar{c})}$ states are close to those predicted in Refs. [30, 40, 46, 51]. Also, our predictions for the $3S$ $T_{(cc\bar{c}\bar{c})}$ states are close to those predicted in Ref. [40]. The predicted masses for the $T_{(bb\bar{b}\bar{b})}$ states in our work are systematically (~ 100 MeV) higher than the results from Refs. [40, 46].

Two $2S$ 0^{++} states $T_{(cc\bar{c}\bar{c})0^{++}}(6908)$ and $T_{(cc\bar{c}\bar{c})0^{++}}(6957)$ and one 2^{++} state $T_{(cc\bar{c}\bar{c})0^{++}}(6927)$ may be candidates of the narrow structure $X(6900)$ recently observed at LHCb in the di- J/ψ invariant mass spectrum [1]. Their masses are very close to that of $X(6900)$, and they can decay via a S -wave mode $J/\psi J/\psi$. The highest 0^{++} $2S$ state $T_{(cc\bar{c}\bar{c})0^{++}}(7185)$ and one low-lying $3S$ states $T_{(cc\bar{c}\bar{c})0^{++}}(7240)$ ($3^3S_{0^{++}(\bar{3}\bar{3})_c(\xi_3)}$) may contribute to the vague structure $X(7200)$ observed at LHCb in the di- J/ψ invariant mass spectrum [1]. It should be mentioned that the $2S$ $T_{(cc\bar{c}\bar{c})0^{++}}(7185)$ state is nearly a pure configuration of $2^1S_{0^{++}(\bar{6}\bar{6})_c(\xi_3)}$, with the color structure $|\bar{6}\bar{6}\rangle_c$ and the radial excitation between diquark (qq) and antiquark ($\bar{q}\bar{q}$). The special color structure of $T_{(cc\bar{c}\bar{c})0^{++}}(7185)$ leads to a rather large mass gap $\Delta \simeq 167$ MeV from the nearby $T_{(cc\bar{c}\bar{c})0^{++}}(7018)$. The large mass splitting between the $2^1S_{0^{++}(\bar{6}\bar{6})_c(\xi_3)}$ and the other 0^{++} configurations are also found in the $ss\bar{s}\bar{s}$ and $bb\bar{b}\bar{b}$ families.

Since the predicted masses for the radially excited $T_{(cc\bar{c}\bar{c})}/T_{(bb\bar{b}\bar{b})}$ states are far above the low-lying two-charmonium/two-bottomonium mass thresholds, most of these $2S$ and $3S$ $T_{(cc\bar{c}\bar{c})}$ and $T_{(bb\bar{b}\bar{b})}$ states could be rather broad since they may easily fall apart and decay into two heavy quarkonium channels. Quantitative study of their decays is crucial for better understanding the properties of these radially excited $T_{(cc\bar{c}\bar{c})}$ and $T_{(bb\bar{b}\bar{b})}$ states.

B. $1D$ states

In the 80 $1D$ -wave states, apart from the conventional quantum numbers, i.e., $J^{PC} = 0^{++}, 1^{++}, 1^{+-}, 2^{++}, 3^{++}, 3^{+-}$ and 4^{++} , there are exotic quantum numbers, i.e., $J^{PC} = 0^{+-}, 2^{+-}$

and 4^{+-} , can be accessed. From the results listed in Tables VII and VIII, it shows that there often exist configuration mixings among the states with the same J^{PC} numbers due to the Coulomb-type potential, linear-confinement potential, and/or spin-spin interactions. For example, two 0^{++} configurations $1^3P_{0^{++}(\bar{6}\bar{6})_c(\xi_1\xi_3, \xi_2\xi_3)}$ and $1^3P_{0^{++}(\bar{3}\bar{3})_c(\xi_1\xi_3, \xi_2\xi_3)}$ are strongly mixed with each other by both the Coulomb-type and linear-confinement potentials. A strong mixing between the two configurations $1^{++} 1^3S_{1^{++}(\bar{6}\bar{6})_c(\xi_1\xi_3, \xi_2\xi_3)}$ and $1^3S_{1^{++}(\bar{3}\bar{3})_c(\xi_1\xi_3, \xi_2\xi_3)}$ is mainly due to the Coulomb-type and spin-spin interactions. It should be mentioned that the effects of the tensor and the spin-orbit interactions are rather small in the configuration mixings among the $1D$ -wave states due to the suppression of the heavy quark masses.

From Tables XIII-XVI, it shows that in the two $L = 0$ (or $L = 1$) configurations containing the same J^{PC} quantum numbers and excitation mode ($\xi_1\xi_3, \xi_2\xi_3$), the low mass configuration has a $|\bar{6}\bar{6}\rangle_c$ structure. In contrast, in the two $L = 2$ configurations containing the same J^{PC} quantum numbers and excitation mode ($\xi_1\xi_3, \xi_2\xi_3$), the low mass configuration has a $|\bar{3}\bar{3}\rangle_c$ structure. For example, in the two 0^{+-} $T_{(cc\bar{c}\bar{c})}$ configurations $1^3P_{0^{+-}(\bar{6}\bar{6})_c(\xi_1\xi_3, \xi_2\xi_3)}$ and $1^3P_{0^{+-}(\bar{3}\bar{3})_c(\xi_1\xi_3, \xi_2\xi_3)}$, the former has a low mass 6868 MeV due to the strong attraction from the Coulomb type potential $\langle V^{Coul} \rangle$ together with the relatively smaller contributions from the linear confinement potential $\langle V^{Lin} \rangle$. For the two 1^{++} $T_{cc\bar{c}\bar{c}}$ configurations with $L = 2$, the mass of $1^3D_{1^{++}(\bar{6}\bar{6})_c(\xi_1\xi_3, \xi_2\xi_3)}$ ($M = 7096$ MeV) turns out to be larger than that of $1^3D_{1^{++}(\bar{3}\bar{3})_c(\xi_1\xi_3, \xi_2\xi_3)}$ ($M = 7028$ MeV). It should be mentioned that in the $L = 0$ (or $L = 1$) configurations, a $|\bar{6}\bar{6}\rangle_c$ structure has larger attractions from the Coulomb type potential than $|\bar{3}\bar{3}\rangle_c$ although all of the color factors $\langle \lambda_i \cdot \lambda_j \rangle$ are negative for $|\bar{3}\bar{3}\rangle_c$. The reason is that for a $|\bar{6}\bar{6}\rangle_c$ structure the color factors $\langle \lambda_1 \cdot \lambda_3 \rangle = \langle \lambda_2 \cdot \lambda_4 \rangle = \langle \lambda_1 \cdot \lambda_4 \rangle = \langle \lambda_2 \cdot \lambda_3 \rangle = -10/3$ are a factor of 2.5 larger than $\langle \lambda_1 \cdot \lambda_3 \rangle = \langle \lambda_2 \cdot \lambda_4 \rangle = \langle \lambda_1 \cdot \lambda_4 \rangle = \langle \lambda_2 \cdot \lambda_3 \rangle = -4/3$ for $|\bar{3}\bar{3}\rangle_c$.

Including configuration mixing effects, the physical masses for the $1D$ -wave $T_{(cc\bar{c}\bar{c})}$ states are predicted to be in the range of $\sim (6700, 7200)$ MeV, and the masses for the $1D$ -wave $T_{(bb\bar{b}\bar{b})}$ states are predicted to be in the range of $\sim (19500, 20000)$ MeV. The mass range for the $1D$ -wave states covers most of the mass range of the $1P$ -wave states and the whole mass range of the $2S$ -wave states. Figure 2 shows that in the mass range $\sim (6700, 7000)$ MeV, many low-lying $1D$ -wave $T_{(cc\bar{c}\bar{c})}$ states highly overlap with the $1P$ -wave states, while in the range of $\sim (6900, 7050)$ MeV, many $1D$ -wave $T_{(cc\bar{c}\bar{c})}$ states highly overlap with the $2S$ -wave states. Such a phenomenon will complicate the experimental analysis if one wants to disentangle their quantum numbers.

For the $T_{(cc\bar{c}\bar{c})}$ sector, the lowest state is the 2^{++} state $T_{(cc\bar{c}\bar{c})2^{++}}(6685)$, which is a mixed state among $1^1D_{2^{++}(\bar{6}\bar{6})_c(\xi_1, \xi_2)}$, $1^1D_{2^{++}(\bar{3}\bar{3})_c(\xi_1, \xi_2)}$, and $1^1D_{2^{++}(\bar{6}\bar{6})_c(\xi_3)}$. In contrast, the highest $T_{(cc\bar{c}\bar{c})}$ state is the 4^{++} state $T_{(cc\bar{c}\bar{c})4^{++}}(7211)$. This state is also a mixed state dominated by the $1^5D_{4^{++}(\bar{3}\bar{3})_c(\xi_3)}$ and $1^5D_{4^{++}(\bar{6}\bar{6})_c(\xi_1, \xi_2)}$ configurations. As shown by the numerical results for $T_{(cc\bar{c}\bar{c})2^{++}}(6685)$ and $T_{(cc\bar{c}\bar{c})4^{++}}(7211)$, the configuration mixing effects can strongly shift the masses of the pure configurations to the physical masses. The mass gap between the lowest mass state $T_{(cc\bar{c}\bar{c})2^{++}}(6685)$ and the highest mass state

$T_{(cc\bar{c}\bar{c})4^{++}}(7211)$ reaches up to a large value of ~ 530 MeV as a combined effect due to the quark interactions. The ξ_3 excitation mode is found to mix significantly with the ξ_1 and ξ_2 excitation modes, and this configuration generally dominates the lowest mass state.

In the D -wave $T_{(cc\bar{c}\bar{c})}$ states, three 0^{++} states $T_{(cc\bar{c}\bar{c})0^{++}}(6833)$, $T_{(cc\bar{c}\bar{c})0^{++}}(6848)$ and $T_{(cc\bar{c}\bar{c})0^{++}}(6962)$, two 1^{++} states $T_{(cc\bar{c}\bar{c})1^{++}}(6851)$ and $T_{(cc\bar{c}\bar{c})1^{++}}(6963)$, three 2^{++} states $T_{(cc\bar{c}\bar{c})2^{++}}(6832)$, $T_{(cc\bar{c}\bar{c})2^{++}}(6857)$ and $T_{(cc\bar{c}\bar{c})2^{++}}(6924)$, one 3^{++} state $T_{(cc\bar{c}\bar{c})3^{++}}(6863)$, and one 4^{++} state $T_{(cc\bar{c}\bar{c})4^{++}}(6870)$ may be candidates of the $X(6900)$ recently observed at LHCb in the di- J/ψ invariant mass spectrum [1]. Their masses are close to that of $X(6900)$, and they can decay into the $J/\psi J/\psi$ channel. It should be mentioned that the $T_{(cc\bar{c}\bar{c})3^{++}}(6863)$ and $T_{(cc\bar{c}\bar{c})4^{++}}(6870)$ are higher J states, and decay into the $J/\psi J/\psi$ channel via a D -wave mode. Thus, their decays into $J/\psi J/\psi$ could be suppressed by the centrifugal barrier and they may appear to be relatively narrow states.

The vague structure $X(7200)$ observed at LHCb in the di- J/ψ invariant mass spectrum [1] may be caused by the high-lying D -wave states with $J^{PC} = 0^{++}, 1^{++}, 2^{++}, 3^{++},$ or 4^{++} . From Fig. 2 it shows that one $J^{PC} = 0^{++}$ state $T_{(cc\bar{c}\bar{c})0^{++}}(7136)$, two $J^{PC} = 1^{++}$ states $T_{(cc\bar{c}\bar{c})1^{++}}(7141, 7146)$, four $J^{PC} = 2^{++}$ states $T_{(cc\bar{c}\bar{c})2^{++}}(7151, 7155, 7165, 7178)$, two 3^{++} states $T_{(cc\bar{c}\bar{c})3^{++}}(7170, 7189)$, and one 4^{++} state $T_{(cc\bar{c}\bar{c})4^{++}}(7211)$ just lie in the vicinity of $X(7200)$. Note that some of these states, e.g. $T_{(cc\bar{c}\bar{c})0^{++}}(7136)$, can fall apart and decay into $J/\psi J/\psi$ via the quark rearrangements. This may suggest that the $X(7200)$ may be originated from nontrivial mechanisms.

IV. SUMMARY

In this work, we further calculate the higher mass spectra for $2S$ -, $3S$ -, and $1D$ -wave fully charmed and bottom tetraquark states in a nonrelativistic potential quark model, which is a continuation of our previous study of the $1S$ - and $1P$ -wave states [28, 32].

Our calculation suggests that within the range of $\sim (6.9, 7.2)$ GeV, it scatters the $2S$ -wave fully-charmed $T_{(cc\bar{c}\bar{c})}$ states, while the $3S$ -wave fully-charmed $T_{(cc\bar{c}\bar{c})}$ states lie in the mass range of $\sim (7.2, 7.4)$ GeV with one 0^{++} state $T_{(cc\bar{c}\bar{c})0^{++}}(7720)$ locating at a mass of $M = 7720$ MeV. We also find that the masses for the $1D$ -wave $T_{(cc\bar{c}\bar{c})}$ states are located in the range of $\sim (6.7, 7.2)$ GeV. Notice that this is also the mass region that $1P$ -wave states sit [32]. We actually obtain a busy spectrum for the fully-charmed tetraquark states with the low-excitation quantum numbers. Similar phenomenon occurs for the fully bottomed tetraquark states which can be seen in Fig. 3.

Our study shows that both the kinetic energy $\langle T \rangle$ and the linear confinement potential $\langle V^{Lin} \rangle$ contribute a large positive value to the tetraquark masses, while the Coulomb type potential $\langle V^{Coul} \rangle$ has a large cancellation with the these two terms. Although some $2S/3S$ and $1D$ configurations have a similar mass, the contributions of $\langle T \rangle$, $\langle V^{Lin} \rangle$ and $\langle V^{Coul} \rangle$ are usually very different from each other. As a consequence of these in-

teractions, most of the physical states are mixing states with different configurations.

The narrow structure $X(6900)$ may be explained by the $1P$ -, or $2S$ -, or $1D$ -wave $T_{(cc\bar{c}\bar{c})}$ states. Within the $1P$ -wave states, our previous study shows that $T_{(cc\bar{c}\bar{c})0^{++}}(6891)$, $T_{(cc\bar{c}\bar{c})1^{++}}(6908)$, and $T_{(cc\bar{c}\bar{c})2^{++}}(6928)$ are possible candidates of $X(6900)$ by looking at the mass locations. In the sector of the $2S$ -wave states, three low-lying states $T_{(cc\bar{c}\bar{c})0^{++}}(6908)$, $T_{(cc\bar{c}\bar{c})0^{++}}(6957)$, and $T_{(cc\bar{c}\bar{c})2^{++}}(6927)$ may contribute to the narrow structure $X(6900)$. In the $1D$ -wave states, three 0^{++} states $T_{(cc\bar{c}\bar{c})0^{++}}(6833, 6848, 6962)$, two 1^{++} states $T_{(cc\bar{c}\bar{c})1^{++}}(6851, 6963)$, three 2^{++} states $T_{(cc\bar{c}\bar{c})2^{++}}(6832, 6857, 6924)$, one 3^{++} state $T_{(cc\bar{c}\bar{c})3^{++}}(6863)$, and one 4^{++} state $T_{(cc\bar{c}\bar{c})4^{++}}(6870)$ may be possible candidates for $X(6900)$.

The vague structure $X(7200)$ may be produced by the highest $2S$ -wave state $T_{(cc\bar{c}\bar{c})0^{++}}(7185)$, two low-lying $3S$ -wave states $T_{(cc\bar{c}\bar{c})0^{++}}(7240)$ and $T_{(cc\bar{c}\bar{c})2^{++}}(7248)$, or several high-lying $1D$ -wave with masses ~ 7.2 GeV and $J^{PC} = 0^{++}, 1^{++}, 2^{++}, 3^{++}, 4^{++}$. It should be mentioned that the $2P$ -wave $T_{(cc\bar{c}\bar{c})}$ states may cover the mass region of $X(7200)$ as well. Unfortunately, in this work we cannot give predictions of the $2P$ -wave spectrum due to its complexity.

To summarize, we have carried out quantitative calculations of the fully-heavy charmed and bottom tetraquark states in order to gain insights into the four-body system with equal-mass heavy quarks and antiquarks. We disentangle the important role played by the confinement potential which implies that the fully-heavy tetraquark states should exist above two heavy quarkonium thresholds. Meanwhile, we find that the potential quark model will predict an extremely rich spectrum with significant configuration mixings. This raises questions on the understanding of the experimental observations since apparently only a few states have been seen in experiment. It should be noted that the rich spectrum predicted in the quark model may be significantly affected by the strong S -wave couplings to the nearby open channels. A combined analysis of the role played by the nearby S -wave continuum channels should be the direction for a better understanding of the multi-quark dynamics in the future. Moreover, to uncover the nature of the structures observed in the di- J/ψ invariant mass spectrum, further studies of the decays of these candidates of $T_{(cc\bar{c}\bar{c})}$ states are desired.

Acknowledgement

This work is supported by the National Natural Science Foundation of China (Grants Nos. U1832173, 11775078, 12175065, 11425525, and 11521505). Q.Z. is also supported in part, by the DFG and NSFC funds to the Sino-German CRC 110 ‘‘Symmetries and the Emergence of Structure in QCD’’ (NSFC Grant No. 12070131001), the Strategic Priority Research Program of Chinese Academy of Sciences (Grant No. XDB34030302), and National Key Basic Research Program of China under Contract No. 2015CB856700.

TABLE II: Configurations for the NS -wave tetraquark $qq\bar{q}\bar{q}$ system, where $N = n + 1$ ($n = 1, 2, \dots$). ξ_1, ξ_2, ξ_3 are the Jacobi coordinates. (ξ_1, ξ_2) stands for a configuration containing both ξ_1 - and ξ_2 -mode excitations.

J^{PC}	Configuration	Wave function
0^{+-}	$N^1 S_{0^{+-}(6\bar{6})_c(\xi_1, \xi_2)}$	$\sqrt{\frac{1}{2}} (\psi_{n00}^{\xi_1} - \psi_{n00}^{\xi_2}) \chi_{00}^{00} 6\bar{6}\rangle^c$
	$N^1 S_{0^{+-}(\bar{3}3)_c(\xi_1, \xi_2)}$	$\sqrt{\frac{1}{2}} (\psi_{n00}^{\xi_1} - \psi_{n00}^{\xi_2}) \chi_{00}^{11} \bar{3}3\rangle^c$
0^{++}	$N^1 S_{0^{++}(6\bar{6})_c(\xi_1, \xi_2)}$	$\sqrt{\frac{1}{2}} (\psi_{n00}^{\xi_1} + \psi_{n00}^{\xi_2}) \chi_{00}^{00} 6\bar{6}\rangle^c$
	$N^1 S_{0^{++}(\bar{3}3)_c(\xi_1, \xi_2)}$	$\sqrt{\frac{1}{2}} (\psi_{n00}^{\xi_1} + \psi_{n00}^{\xi_2}) \chi_{00}^{11} \bar{3}3\rangle^c$
	$N^1 S_{0^{++}(6\bar{6})_c(\xi_3)}$	$\psi_{n00}^{\xi_3} \chi_{00}^{00} 6\bar{6}\rangle^c$
	$N^1 S_{0^{++}(\bar{3}3)_c(\xi_3)}$	$\psi_{n00}^{\xi_3} \chi_{00}^{11} \bar{3}3\rangle^c$
1^{+-}	$N^3 S_{1^{+-}(\bar{3}3)_c(\xi_1, \xi_2)}$	$\sqrt{\frac{1}{2}} (\psi_{n00}^{\xi_1} + \psi_{n00}^{\xi_2}) \chi_{11}^{11} \bar{3}3\rangle^c$
	$N^3 S_{1^{+-}(\bar{3}3)_c(\xi_3)}$	$\psi_{n00}^{\xi_3} \chi_{11}^{11} \bar{3}3\rangle^c$
1^{++}	$N^3 S_{1^{++}(\bar{3}3)_c(\xi_1, \xi_2)}$	$\sqrt{\frac{1}{2}} (\psi_{n00}^{\xi_1} - \psi_{n00}^{\xi_2}) \chi_{11}^{11} \bar{3}3\rangle^c$
2^{+-}	$N^5 S_{2^{+-}(\bar{3}3)_c(\xi_1, \xi_2)}$	$\sqrt{\frac{1}{2}} (\psi_{n00}^{\xi_1} - \psi_{n00}^{\xi_2}) \chi_{22}^{11} \bar{3}3\rangle^c$
	$N^5 S_{2^{++}(\bar{3}3)_c(\xi_1, \xi_2)}$	$\sqrt{\frac{1}{2}} (\psi_{n00}^{\xi_1} + \psi_{n00}^{\xi_2}) \chi_{22}^{11} \bar{3}3\rangle^c$
2^{++}	$N^5 S_{2^{++}(\bar{3}3)_c(\xi_3)}$	$\psi_{n00}^{\xi_3} \chi_{22}^{11} \bar{3}3\rangle^c$

- [1] R. Aaij *et al.* [LHCb Collaboration], Observation of structure in the J/ψ -pair mass spectrum, *Sci. Bull.* **65**, no. 23, 1983 (2020).
- [2] K. T. Chao and S. L. Zhu, The possible tetraquark states $cc\bar{c}\bar{c}$ observed by the LHCb experiment, *Sci. Bull.* **65**, no. 23, 1952 (2020).
- [3] J. M. Richard, About the J/ψ J/ψ peak of LHCb: fully-charmed tetraquark?, *Sci. Bull.* **65**, 1954 (2020).
- [4] Y. Iwasaki, A possible model for new resonances-exotics and hidden charm, *Prog. Theor. Phys.* **54**, 492 (1975).
- [5] S. Zouzou, B. Silvestre-Brac, C. Gignoux and J. M. Richard, Four quark bound states, *Z. Phys. C* **30**, 457 (1986).
- [6] L. Heller and J. A. Tjon, On bound states of heavy $Q^2\bar{Q}^2$ systems, *Phys. Rev. D* **32**, 755 (1985).
- [7] K. T. Chao, The (cc) - $(\bar{c}\bar{c})$ (Diquark-Anti-Diquark) States in e^+e^- Annihilation, *Z. Phys. C* **7**, 317 (1981).
- [8] J. Vijande, A. Valcarce, and N. Barnea, Exotic meson-meson molecules and compact four-quark states, *Phys. Rev. D* **79**, 074010 (2009).
- [9] M. N. Anwar, J. Ferretti, F. K. Guo, E. Santopinto, and B. S. Zou, Spectroscopy and decays of the fully-heavy tetraquarks, *Eur. Phys. J. C* **78**, 647 (2018).
- [10] Y. Bai, S. Lu and J. Osborne, Beauty-full Tetraquarks, *Phys. Lett. B* **798**, 134930 (2019).
- [11] A. V. Berezhnoy, A. V. Luchinsky and A. A. Novoselov, Tetraquarks composed of 4 heavy quarks, *Phys. Rev. D* **86**, 034004 (2012).
- [12] N. Barnea, J. Vijande, and A. Valcarce, Four-quark spectroscopy within the hyperspherical formalism, *Phys. Rev. D* **73**, 054004 (2006).
- [13] Z. G. Wang, Analysis of the $QQ\bar{Q}\bar{Q}$ tetraquark states with QCD sum rules, *Eur. Phys. J. C* **77**, 432 (2017).
- [14] Z. G. Wang and Z. Y. Di, Analysis of the vector and axialvector $QQ\bar{Q}\bar{Q}$ tetraquark states with QCD sum rules, *Acta Phys. Polon. B* **50**, 1335 (2019).
- [15] M. A. Bedolla, J. Ferretti, C. D. Roberts and E. Santopinto, Spectrum of fully-heavy tetraquarks from a diquark+antidiquark perspective, *Eur. Phys. J. C* **80**, 1004 (2020).
- [16] V. R. Debastiani and F. S. Navarra, A non-relativistic model for the $[cc][\bar{c}\bar{c}]$ tetraquark, *Chin. Phys. C* **43**, 013105 (2019).
- [17] A. Esposito and A. D. Polosa, A $bb\bar{b}\bar{b}$ di-bottomonium at the LHC?, *Eur. Phys. J. C* **78**, 782 (2018).
- [18] P. Lundhammar and T. Ohlsson, Nonrelativistic model of tetraquarks and predictions for their masses from fits to charmed and bottom meson data, *Phys. Rev. D* **102**, 054018 (2020).
- [19] J. M. Richard, A. Valcarce, and J. Vijande, Few-body quark dynamics for doubly heavy baryons and tetraquarks, *Phys. Rev. C* **97**, 035211 (2018).
- [20] J. M. Richard, A. Valcarce, and J. Vijande, String dynamics and metastability of all-heavy tetraquarks, *Phys. Rev. D* **95**, 054019 (2017).
- [21] J. Wu, Y. R. Liu, K. Chen, X. Liu, and S. L. Zhu, Heavy-flavored tetraquark states with the $QQ\bar{Q}\bar{Q}$ configuration, *Phys. Rev. D* **97**, 094015 (2018).
- [22] C. Hughes, E. Eichten, and C. T. H. Davies, Searching for beauty-fully bound tetraquarks using lattice nonrelativistic QCD, *Phys. Rev. D* **97**, 054505 (2018).
- [23] M. Karliner, S. Nussinov, and J. L. Rosner, $QQ\bar{Q}\bar{Q}$ states: Masses, production, and decays, *Phys. Rev. D* **95**, 034011 (2017).
- [24] R. J. Lloyd and J. P. Vary, All charm tetraquarks, *Phys. Rev. D* **70**, 014009 (2004).
- [25] J. P. Ader, J. M. Richard and P. Taxil, Do narrow heavy multi-quark states exist, *Phys. Rev. D* **25**, 2370 (1982).
- [26] W. Chen, H. X. Chen, X. Liu, T. G. Steele and S. L. Zhu, Hunting for exotic doubly hidden-charm/bottom tetraquark states, *Phys. Lett. B* **773**, 247 (2017).
- [27] W. Chen, H. X. Chen, X. Liu, T. G. Steele and S. L. Zhu, Doubly hidden-charm/bottom $QQ\bar{Q}\bar{Q}$ tetraquark states, *EPJ Web Conf.* **182**, 02028 (2018).

TABLE V: Predicted mass spectrum for the 2S- and 3S-wave $T_{(cc\bar{c}\bar{c})}$ states.

J^{PC}	Configuration	$\langle H \rangle$ (MeV)	Mass (MeV)	Eigenvector
0^{+-}	$2^1S_{0^{+-}(\bar{66})_c(\xi_1, \xi_2)}$	$\begin{pmatrix} 7008 & -14 \\ -14 & 7005 \end{pmatrix}$	$\begin{pmatrix} 6993 \\ 7020 \end{pmatrix}$	$\begin{pmatrix} -0.66 & -0.75 \\ -0.75 & 0.66 \end{pmatrix}$
	$2^1S_{0^{+-}(\bar{33})_c(\xi_1, \xi_2)}$			
0^{++}	$2^1S_{0^{++}(\bar{66})_c(\xi_1, \xi_2)}$	$\begin{pmatrix} 6954 & -19 & 13 & -11 \\ -19 & 7000 & -4 & -36 \\ 13 & -4 & 7183 & -12 \\ -11 & -36 & -12 & 6930 \end{pmatrix}$	$\begin{pmatrix} 6908 \\ 6957 \\ 7018 \\ 7185 \end{pmatrix}$	$\begin{pmatrix} 0.35 & 0.40 & 0.03 & 0.84 \\ -0.91 & -0.05 & 0.07 & 0.41 \\ 0.21 & -0.91 & -0.01 & 0.35 \\ -0.06 & 0.02 & -1.00 & 0.05 \end{pmatrix}$
	$2^1S_{0^{++}(\bar{33})_c(\xi_1, \xi_2)}$			
	$2^1S_{0^{++}(\bar{66})_c(\xi_3)}$			
	$2^1S_{0^{++}(\bar{33})_c(\xi_3)}$			
1^{+-}	$2^3S_{1^{+-}(\bar{33})_c(\xi_1, \xi_2)}$	$\begin{pmatrix} 7006 & -37 \\ -37 & 6934 \end{pmatrix}$	$\begin{pmatrix} 6919 \\ 7021 \end{pmatrix}$	$\begin{pmatrix} -0.39 & -0.92 \\ -0.92 & 0.39 \end{pmatrix}$
	$2^3S_{1^{+-}(\bar{33})_c(\xi_3)}$			
1^{++}	$2^3S_{1^{++}(\bar{33})_c(\xi_1, \xi_2)}$	$\begin{pmatrix} 7009 \end{pmatrix}$	7009	1
2^{+-}	$2^5S_{2^{+-}(\bar{33})_c(\xi_1, \xi_2)}$	$\begin{pmatrix} 7017 \end{pmatrix}$	7017	1
2^{++}	$2^5S_{2^{++}(\bar{33})_c(\xi_1, \xi_2)}$	$\begin{pmatrix} 7018 & -36 \\ -36 & 6942 \end{pmatrix}$	$\begin{pmatrix} 6927 \\ 7032 \end{pmatrix}$	$\begin{pmatrix} -0.37 & -0.93 \\ -0.93 & 0.37 \end{pmatrix}$
	$2^5S_{2^{++}(\bar{33})_c(\xi_3)}$			
0^{+-}	$3^1S_{0^{+-}(\bar{66})_c(\xi_1, \xi_2)}$	$\begin{pmatrix} 7356 & 9 \\ 9 & 7396 \end{pmatrix}$	$\begin{pmatrix} 7354 \\ 7398 \end{pmatrix}$	$\begin{pmatrix} -0.98 & 0.21 \\ 0.21 & 0.98 \end{pmatrix}$
	$3^1S_{0^{+-}(\bar{33})_c(\xi_1, \xi_2)}$			
0^{++}	$3^1S_{0^{++}(\bar{66})_c(\xi_1, \xi_2)}$	$\begin{pmatrix} 7347 & -10 & 1 & -4 \\ -10 & 7403 & 0 & 2 \\ 1 & 0 & 7720 & -6 \\ -4 & 2 & -6 & 7241 \end{pmatrix}$	$\begin{pmatrix} 7240 \\ 7346 \\ 7405 \\ 7720 \end{pmatrix}$	$\begin{pmatrix} 0.03 & -0.01 & 0.01 & 1.00 \\ -0.99 & -0.17 & 0 & 0.03 \\ 0.17 & -0.99 & 0 & -0.02 \\ 0 & 0 & -1.00 & 0.01 \end{pmatrix}$
	$3^1S_{0^{++}(\bar{33})_c(\xi_1, \xi_2)}$			
	$3^1S_{0^{++}(\bar{66})_c(\xi_3)}$			
	$3^1S_{0^{++}(\bar{33})_c(\xi_3)}$			
1^{+-}	$3^3S_{1^{+-}(\bar{33})_c(\xi_1, \xi_2)}$	$\begin{pmatrix} 7406 & 3 \\ 3 & 7243 \end{pmatrix}$	$\begin{pmatrix} 7243 \\ 7406 \end{pmatrix}$	$\begin{pmatrix} 0.02 & -1.00 \\ -1.00 & -0.02 \end{pmatrix}$
	$3^3S_{1^{+-}(\bar{33})_c(\xi_3)}$			
1^{++}	$3^3S_{1^{++}(\bar{33})_c(\xi_1, \xi_2)}$	$\begin{pmatrix} 7399 \end{pmatrix}$	7399	1
2^{+-}	$3^5S_{2^{+-}(\bar{33})_c(\xi_1, \xi_2)}$	$\begin{pmatrix} 7405 \end{pmatrix}$	7405	1
2^{++}	$3^5S_{2^{++}(\bar{33})_c(\xi_1, \xi_2)}$	$\begin{pmatrix} 7412 & 3 \\ 3 & 7248 \end{pmatrix}$	$\begin{pmatrix} 7248 \\ 7412 \end{pmatrix}$	$\begin{pmatrix} 0.02 & -1.00 \\ -1.00 & -0.02 \end{pmatrix}$
	$3^5S_{2^{++}(\bar{33})_c(\xi_3)}$			

TABLE VI: Predicted mass spectrum for the 2S- and 3S-wave $T_{(bb\bar{b}\bar{b})}$ states.

J^{PC}	Configuration	$\langle H \rangle$ (MeV)	Mass (MeV)	Eigenvector
0^{+-}	$2^1S_{0^{+-}(\bar{66})_c(\xi_1, \xi_2)}$	$\begin{pmatrix} 19840 & 5 \\ 5 & 19790 \end{pmatrix}$	$\begin{pmatrix} 19789 \\ 19841 \end{pmatrix}$	$\begin{pmatrix} 0.10 & -1.00 \\ -1.00 & -0.10 \end{pmatrix}$
	$2^1S_{0^{+-}(\bar{33})_c(\xi_1, \xi_2)}$			
0^{++}	$2^1S_{0^{++}(\bar{66})_c(\xi_1, \xi_2)}$	$\begin{pmatrix} 19770 & -7 & -30 & -4 \\ -7 & 19797 & -1 & -31 \\ -30 & -1 & 19972 & -4 \\ -4 & -31 & -4 & 19733 \end{pmatrix}$	$\begin{pmatrix} 19719 \\ 19767 \\ 19811 \\ 19976 \end{pmatrix}$	$\begin{pmatrix} 0.15 & 0.38 & 0.04 & 0.91 \\ -0.97 & -0.04 & -0.14 & 0.19 \\ 0.10 & -0.92 & 0.02 & 0.37 \\ 0.14 & 0 & -0.99 & 0.01 \end{pmatrix}$
	$2^1S_{0^{++}(\bar{33})_c(\xi_1, \xi_2)}$			
	$2^1S_{0^{++}(\bar{66})_c(\xi_3)}$			
	$2^1S_{0^{++}(\bar{33})_c(\xi_3)}$			
1^{+-}	$2^3S_{1^{+-}(\bar{33})_c(\xi_1, \xi_2)}$	$\begin{pmatrix} 19800 & -32 \\ -32 & 19735 \end{pmatrix}$	$\begin{pmatrix} 19722 \\ 19813 \end{pmatrix}$	$\begin{pmatrix} -0.38 & -0.92 \\ -0.92 & 0.38 \end{pmatrix}$
	$2^3S_{1^{+-}(\bar{33})_c(\xi_3)}$			
1^{++}	$2^3S_{1^{++}(\bar{33})_c(\xi_1, \xi_2)}$	$\begin{pmatrix} 19792 \end{pmatrix}$	19792	1
2^{+-}	$2^5S_{2^{+-}(\bar{33})_c(\xi_1, \xi_2)}$	$\begin{pmatrix} 19795 \end{pmatrix}$	19795	1
2^{++}	$2^5S_{2^{++}(\bar{33})_c(\xi_1, \xi_2)}$	$\begin{pmatrix} 19804 & -31 \\ -31 & 19738 \end{pmatrix}$	$\begin{pmatrix} 19726 \\ 19816 \end{pmatrix}$	$\begin{pmatrix} -0.37 & -0.93 \\ -0.93 & 0.37 \end{pmatrix}$
	$2^5S_{2^{++}(\bar{33})_c(\xi_3)}$			
0^{+-}	$3^1S_{0^{+-}(\bar{66})_c(\xi_1, \xi_2)}$	$\begin{pmatrix} 20128 & 3 \\ 3 & 20115 \end{pmatrix}$	$\begin{pmatrix} 20115 \\ 20129 \end{pmatrix}$	$\begin{pmatrix} 0.21 & -0.98 \\ -0.98 & -0.21 \end{pmatrix}$
	$3^1S_{0^{+-}(\bar{33})_c(\xi_1, \xi_2)}$			
0^{++}	$3^1S_{0^{++}(\bar{66})_c(\xi_1, \xi_2)}$	$\begin{pmatrix} 20120 & -3 & -1 & -1 \\ -3 & 20128 & 0 & 2 \\ -1 & 0 & 20405 & -2 \\ -1 & 2 & -2 & 19979 \end{pmatrix}$	$\begin{pmatrix} 19979 \\ 20119 \\ 20129 \\ 20405 \end{pmatrix}$	$\begin{pmatrix} 0.01 & -0.01 & 0 & 1.00 \\ -0.95 & -0.32 & 0 & 0.01 \\ -0.32 & 0.95 & 0 & 0.01 \\ 0 & 0 & -1.00 & 0 \end{pmatrix}$
	$3^1S_{0^{++}(\bar{33})_c(\xi_1, \xi_2)}$			
	$3^1S_{0^{++}(\bar{66})_c(\xi_3)}$			
	$3^1S_{0^{++}(\bar{33})_c(\xi_3)}$			
1^{+-}	$3^3S_{1^{+-}(\bar{33})_c(\xi_1, \xi_2)}$	$\begin{pmatrix} 20129 & 2 \\ 2 & 19980 \end{pmatrix}$	$\begin{pmatrix} 19980 \\ 20129 \end{pmatrix}$	$\begin{pmatrix} 0.01 & -1.00 \\ -1.00 & -0.01 \end{pmatrix}$
	$3^3S_{1^{+-}(\bar{33})_c(\xi_3)}$			
1^{++}	$3^3S_{1^{++}(\bar{33})_c(\xi_1, \xi_2)}$	$\begin{pmatrix} 20116 \end{pmatrix}$	20116	1
2^{+-}	$3^5S_{2^{+-}(\bar{33})_c(\xi_1, \xi_2)}$	$\begin{pmatrix} 20118 \end{pmatrix}$	20118	1
2^{++}	$3^5S_{2^{++}(\bar{33})_c(\xi_1, \xi_2)}$	$\begin{pmatrix} 20131 & 2 \\ 2 & 19982 \end{pmatrix}$	$\begin{pmatrix} 19982 \\ 20131 \end{pmatrix}$	$\begin{pmatrix} 0.01 & -1.00 \\ -1.00 & -0.01 \end{pmatrix}$
	$3^5S_{2^{++}(\bar{33})_c(\xi_3)}$			

TABLE VII: Predicted mass spectrum for the $1D$ -wave $T_{(ccc\bar{c})}$ states.

J^{PC}	Configuration	$\langle H \rangle$ (MeV)	Mass (MeV)	Eigenvector	
0^{+-}	$1^3P_{0^{++}(66)_c}(\xi_1\xi_3, \xi_2\xi_3)$	$\begin{pmatrix} 6868 & -113 \\ -113 & 6948 \end{pmatrix}$	$\begin{pmatrix} 6788 \\ 7028 \end{pmatrix}$	$\begin{pmatrix} -0.82 & -0.58 \\ -0.58 & 0.82 \end{pmatrix}$	
	$1^5D_{0^{++}(33)_c}(\xi_1, \xi_2)$	$\begin{pmatrix} 7054 \end{pmatrix}$	7054	1	
	$1^1S_{0^{++}(33)_c}(\xi_1\xi_2)$	$\begin{pmatrix} 6838 \end{pmatrix}$	6838	1	
0^{++}	$1^1S_{0^{++}(66)_c}(\xi_1\xi_2)$	$\begin{pmatrix} 6957 \end{pmatrix}$	6957	1	
	$1^3P_{0^{++}(6\bar{6})_c}(\xi_1\xi_3, \xi_2\xi_3)$	$\begin{pmatrix} 6857 & 136 \\ 136 & 6944 \end{pmatrix}$	$\begin{pmatrix} 6758 \\ 7043 \end{pmatrix}$	$\begin{pmatrix} -0.81 & 0.59 \\ 0.59 & 0.81 \end{pmatrix}$	
	$1^3P_{0^{++}(\bar{3}3)_c}(\xi_1\xi_3, \xi_2\xi_3)$	$\begin{pmatrix} 7053 \end{pmatrix}$	7053	1	
	$1^5D_{0^{++}(33)_c}(\xi_1, \xi_2)$	$\begin{pmatrix} 7051 & 61 & 6 \\ 61 & 6968 & -128 \\ 6 & -128 & 7013 \end{pmatrix}$	$\begin{pmatrix} 7048 \\ 6848 \\ 7136 \end{pmatrix}$	$\begin{pmatrix} 0.88 & -0.09 & 0.47 \\ -0.25 & 0.76 & 0.6 \\ 0.41 & 0.64 & -0.65 \end{pmatrix}$	
	$1^5D_{0^{++}(\bar{3}3)_c}(\xi_3)$				
	$1^5D_{0^{++}(6\bar{6})_c}(\xi_1\xi_2)$				
	$1^3S_{1^{+-}(66)_c}(\xi_1\xi_3, \xi_2\xi_3)$	$\begin{pmatrix} 7002 & -7 \\ -7 & 7007 \end{pmatrix}$	$\begin{pmatrix} 6997 \\ 7012 \end{pmatrix}$	$\begin{pmatrix} -0.82 & -0.58 \\ -0.58 & 0.82 \end{pmatrix}$	
1^{+-}	$1^3S_{1^{+-}(33)_c}(\xi_1\xi_3, \xi_2\xi_3)$	$\begin{pmatrix} 6973 \end{pmatrix}$	6973	1	
	$1^1P_{1^{+-}(33)_c}(\xi_1\xi_2)$	$\begin{pmatrix} 6871 \end{pmatrix}$	6871	1	
	$1^1P_{1^{+-}(6\bar{6})_c}(\xi_1\xi_2)$	$\begin{pmatrix} 7052 \end{pmatrix}$	7052	1	
	$1^3P_{1^{+-}(66)_c}(\xi_1\xi_3, \xi_2\xi_3)$	$\begin{pmatrix} 6867 & -112 \\ -112 & 6946 \end{pmatrix}$	$\begin{pmatrix} 6788 \\ 7025 \end{pmatrix}$	$\begin{pmatrix} -0.82 & -0.58 \\ -0.58 & 0.82 \end{pmatrix}$	
	$1^3P_{1^{+-}(\bar{3}3)_c}(\xi_1\xi_3, \xi_2\xi_3)$	$\begin{pmatrix} 7069 \end{pmatrix}$	7069	1	
	$1^5P_{1^{+-}(66)_c}(\xi_1\xi_2)$	$\begin{pmatrix} 7062 & 0 & 18 \\ 0 & 6978 & -142 \\ 18 & -142 & 7008 \end{pmatrix}$	$\begin{pmatrix} 6833 \\ 7066 \\ 7149 \end{pmatrix}$	$\begin{pmatrix} 0.26 & -0.73 & -0.62 \\ -0.88 & 0.08 & -0.46 \\ 0.39 & 0.67 & -0.63 \end{pmatrix}$	
	$1^3D_{1^{+-}(33)_c}(\xi_3)$				
	$1^3D_{1^{+-}(6\bar{6})_c}(\xi_1\xi_2)$				
	$1^3D_{1^{+-}(66)_c}(\xi_1\xi_3, \xi_2\xi_3)$	$\begin{pmatrix} 7092 & 93 \\ 93 & 7026 \end{pmatrix}$	$\begin{pmatrix} 7158 \\ 6960 \end{pmatrix}$	$\begin{pmatrix} -0.82 & -0.58 \\ 0.58 & -0.82 \end{pmatrix}$	
	$1^3D_{1^{+-}(\bar{3}3)_c}(\xi_1\xi_3, \xi_2\xi_3)$	$\begin{pmatrix} 7064 \end{pmatrix}$	7064	1	
	$1^5D_{1^{+-}(33)_c}(\xi_1, \xi_2)$				
	1^{++}	$1^3S_{1^{++}(66)_c}(\xi_1\xi_3, \xi_2\xi_3)$	$\begin{pmatrix} 6991 & 34 \\ 34 & 7003 \end{pmatrix}$	$\begin{pmatrix} 6962 \\ 7032 \end{pmatrix}$	$\begin{pmatrix} -0.77 & 0.64 \\ 0.64 & 0.77 \end{pmatrix}$
		$1^3S_{1^{++}(33)_c}(\xi_1\xi_3, \xi_2\xi_3)$	$\begin{pmatrix} 6861 & 140 \\ 140 & 6944 \end{pmatrix}$	$\begin{pmatrix} 6756 \\ 7049 \end{pmatrix}$	$\begin{pmatrix} -0.80 & 0.60 \\ 0.60 & 0.80 \end{pmatrix}$
$1^3P_{1^{++}(66)_c}(\xi_1\xi_3, \xi_2\xi_3)$		$\begin{pmatrix} 7051 \end{pmatrix}$	7051	1	
$1^3P_{1^{++}(\bar{3}3)_c}(\xi_1\xi_3, \xi_2\xi_3)$		$\begin{pmatrix} 7070 \end{pmatrix}$	7070	1	
$1^3D_{1^{++}(66)_c}(\xi_1\xi_3, \xi_2\xi_3)$		$\begin{pmatrix} 7096 & -69 \\ -69 & 7028 \end{pmatrix}$	$\begin{pmatrix} 7139 \\ 6985 \end{pmatrix}$	$\begin{pmatrix} -0.85 & 0.53 \\ -0.53 & -0.85 \end{pmatrix}$	
$1^3D_{1^{++}(\bar{3}3)_c}(\xi_1\xi_3, \xi_2\xi_3)$		$\begin{pmatrix} 7059 & 62 & 10 \\ 62 & 6976 & -132 \\ 10 & -132 & 7022 \end{pmatrix}$	$\begin{pmatrix} 7060 \\ 6851 \\ 7146 \end{pmatrix}$	$\begin{pmatrix} 0.89 & -0.06 & 0.46 \\ -0.25 & 0.76 & 0.6 \\ 0.38 & 0.65 & -0.66 \end{pmatrix}$	
$1^5D_{1^{++}(33)_c}(\xi_3)$					
$1^5D_{1^{++}(6\bar{6})_c}(\xi_1\xi_2)$					
$1^3P_{2^{+-}(66)_c}(\xi_1\xi_3, \xi_2\xi_3)$		$\begin{pmatrix} 6873 & -121 \\ -121 & 6959 \end{pmatrix}$	$\begin{pmatrix} 6788 \\ 7044 \end{pmatrix}$	$\begin{pmatrix} 0.82 & 0.58 \\ -0.58 & 0.82 \end{pmatrix}$	
2^{+-}		$1^3P_{2^{+-}(\bar{3}3)_c}(\xi_1\xi_3, \xi_2\xi_3)$	$\begin{pmatrix} 7072 \end{pmatrix}$	7072	1
	$1^1D_{2^{+-}(66)_c}(\xi_1, \xi_2)$	$\begin{pmatrix} 6985 \end{pmatrix}$	6985	1	
	$1^1D_{2^{+-}(\bar{3}3)_c}(\xi_1, \xi_2)$	$\begin{pmatrix} 7087 \end{pmatrix}$	7087	1	
	$1^3D_{2^{+-}(33)_c}(\xi_1, \xi_2)$	$\begin{pmatrix} 7073 & 70 & 26 \\ 70 & 6985 & -149 \\ 26 & -149 & 7028 \end{pmatrix}$	$\begin{pmatrix} 6835 \\ 7085 \\ 7166 \end{pmatrix}$	$\begin{pmatrix} -0.28 & 0.74 & 0.61 \\ 0.90 & -0.01 & 0.43 \\ 0.32 & 0.67 & -0.67 \end{pmatrix}$	
	$1^3D_{2^{+-}(\bar{3}3)_c}(\xi_3)$				
	$1^3D_{2^{+-}(6\bar{6})_c}(\xi_1\xi_2)$				
	$1^3D_{2^{+-}(66)_c}(\xi_1\xi_3, \xi_2\xi_3)$	$\begin{pmatrix} 7106 & 86 \\ 86 & 7045 \end{pmatrix}$	$\begin{pmatrix} 7167 \\ 6984 \end{pmatrix}$	$\begin{pmatrix} 0.82 & 0.58 \\ -0.58 & 0.82 \end{pmatrix}$	
	$1^3D_{2^{+-}(\bar{3}3)_c}(\xi_1\xi_3, \xi_2\xi_3)$	$\begin{pmatrix} 7082 \end{pmatrix}$	7082	1	
	$1^5D_{2^{+-}(\bar{3}3)_c}(\xi_1, \xi_2)$				

- [28] M. S. Liu, Q. F. Lü, X. H. Zhong and Q. Zhao, All-heavy tetraquarks, Phys. Rev. D **100**, 016006 (2019).
[29] C. Deng, H. Chen and J. Ping, Towards the understanding of fully-heavy tetraquark states from various models, Phys. Rev. D **103**, 014001 (2021).
[30] G. J. Wang, L. Meng and S. L. Zhu, Spectrum of the fully-heavy tetraquark state $QQ\bar{Q}'\bar{Q}'$, Phys. Rev. D **100**, 096013 (2019).

- [31] X. Chen, Fully-charm tetraquarks: $cc\bar{c}\bar{c}$, arXiv:2001.06755 [hep-ph].
[32] M. S. Liu, F. X. Liu, X. H. Zhong and Q. Zhao, Full-heavy tetraquark states and their evidences in the LHCb di- J/ψ spectrum, arXiv:2006.11952 [hep-ph].
[33] Q. Li, C. H. Chang, G. L. Wang and T. Wang, Mass spectra and wave functions of $T_{QQ\bar{Q}\bar{Q}}$ tetraquarks, Phys. Rev. D **104**, 014018

TABLE VIII: Predicted mass spectrum for the $1D$ -wave $T_{(ccc\bar{c})}$ states (Continued).

J^{PC}	Configuration	$\langle H \rangle$ (MeV)	Mass (MeV)	Eigenvector
2^{++}	$1^5S_{2^{++}(6\bar{6})_c(\xi_1\xi_2)}$	(7004)	7004	1
	$1^3P_{2^{++}(6\bar{6})_c(\xi_1\xi_3\xi_2\xi_3)}$	$\begin{pmatrix} 6864 & 145 \\ 145 & 6955 \end{pmatrix}$	$\begin{pmatrix} 6758 \\ 7061 \end{pmatrix}$	$\begin{pmatrix} -0.81 & 0.59 \\ 0.59 & 0.81 \end{pmatrix}$
	$1^3P_{2^{++}(3\bar{3})_c(\xi_1\xi_3\xi_2\xi_3)}$	(7073)	7073	1
	$1^1D_{2^{++}(6\bar{6})_c(\xi_1\xi_2)}$	$\begin{pmatrix} 6955 & -19 & 174 & 5 & 25 & 3 \\ -19 & 7073 & 5 & 72 & 1 & 28 \\ 174 & 5 & 6964 & -21 & -147 & -6 \\ 5 & 72 & -21 & 6986 & -2 & -153 \\ 25 & 1 & -147 & -2 & 6859 & -20 \\ 3 & 28 & -6 & -153 & -20 & 7018 \end{pmatrix}$	$\begin{pmatrix} 7151 \\ 7086 \\ 6685 \\ 6832 \\ 6924 \\ 7178 \end{pmatrix}$	$\begin{pmatrix} -0.45 & -0.17 & -0.55 & -0.45 & 0.21 & 0.46 \\ 0.03 & -0.9 & -0.08 & 0.02 & 0.09 & -0.42 \\ 0.46 & 0.06 & -0.62 & -0.13 & -0.6 & -0.12 \\ -0.09 & 0.28 & 0.1 & -0.72 & 0.13 & -0.61 \\ -0.65 & -0.08 & 0.21 & 0.01 & -0.72 & -0.07 \\ -0.38 & 0.28 & -0.5 & 0.51 & 0.23 & -0.46 \end{pmatrix}$
	$1^1D_{2^{++}(3\bar{3})_c(\xi_3)}$		6685	
	$1^1D_{2^{++}(3\bar{3})_c(\xi_3)}$		6832	
	$1^1D_{2^{++}(3\bar{3})_c(\xi_1\xi_2)}$		6924	
	$1^1D_{2^{++}(6\bar{6})_c(\xi_1\xi_2)}$		7178	
	$1^3D_{2^{++}(3\bar{3})_c(\xi_1\xi_2)}$	(7085)	7085	1
	$1^3D_{2^{++}(6\bar{6})_c(\xi_1\xi_3\xi_2\xi_3)}$	$\begin{pmatrix} 7105 & -74 \\ -74 & 7045 \end{pmatrix}$	$\begin{pmatrix} 7155 \\ 6995 \end{pmatrix}$	$\begin{pmatrix} -0.83 & 0.56 \\ 0.56 & 0.83 \end{pmatrix}$
	$1^3D_{2^{++}(3\bar{3})_c(\xi_1\xi_3\xi_2\xi_3)}$		6995	
	$1^5D_{2^{++}(3\bar{3})_c(\xi_1\xi_2)}$	$\begin{pmatrix} 7073 & 65 & 17 \\ 65 & 6989 & -138 \\ 17 & -138 & 7040 \end{pmatrix}$	$\begin{pmatrix} 7080 \\ 6857 \\ 7165 \end{pmatrix}$	$\begin{pmatrix} -0.90 & 0.02 & -0.43 \\ -0.27 & 0.76 & 0.59 \\ -0.34 & -0.65 & 0.68 \end{pmatrix}$
	$1^5D_{2^{++}(3\bar{3})_c(\xi_3)}$		6857	
	$1^5D_{2^{++}(6\bar{6})_c(\xi_1\xi_2)}$		7165	
	3^{+-}	$1^5P_{3^{+-}(6\bar{6})_c(\xi_1\xi_2)}$	(7102)	7102
$1^3D_{3^{+-}(3\bar{3})_c(\xi_1\xi_2)}$		$\begin{pmatrix} 7089 & 73 & 31 \\ 73 & 7002 & -154 \\ 31 & -154 & 7043 \end{pmatrix}$	$\begin{pmatrix} 6844 \\ 7105 \\ 7186 \end{pmatrix}$	$\begin{pmatrix} -0.30 & 0.73 & 0.61 \\ 0.91 & 0.01 & 0.42 \\ 0.30 & 0.68 & -0.67 \end{pmatrix}$
$1^3D_{3^{+-}(3\bar{3})_c(\xi_3)}$			7105	
$1^3D_{3^{+-}(6\bar{6})_c(\xi_1\xi_2)}$			7186	
$1^3D_{3^{+-}(6\bar{6})_c(\xi_1\xi_3\xi_2\xi_3)}$		$\begin{pmatrix} 7124 & 87 \\ 87 & 7062 \end{pmatrix}$	$\begin{pmatrix} 7185 \\ 7001 \end{pmatrix}$	$\begin{pmatrix} -0.82 & -0.58 \\ 0.58 & -0.82 \end{pmatrix}$
$1^3D_{3^{+-}(3\bar{3})_c(\xi_1\xi_3\xi_2\xi_3)}$			7001	
$1^5D_{3^{+-}(3\bar{3})_c(\xi_1\xi_2)}$		(7103)	7103	1
3^{++}	$1^3D_{3^{++}(3\bar{3})_c(\xi_1\xi_2)}$	(7103)	7103	1
	$1^3D_{3^{++}(6\bar{6})_c(\xi_1\xi_3\xi_2\xi_3)}$	$\begin{pmatrix} 7126 & -69 \\ -69 & 7063 \end{pmatrix}$	$\begin{pmatrix} 7170 \\ 7019 \end{pmatrix}$	$\begin{pmatrix} 0.84 & -0.54 \\ 0.54 & 0.84 \end{pmatrix}$
	$1^3D_{3^{++}(3\bar{3})_c(\xi_1\xi_3\xi_2\xi_3)}$		7019	
	$1^5D_{3^{++}(3\bar{3})_c(\xi_1\xi_2)}$	$\begin{pmatrix} 7091 & 69 & 25 \\ 69 & 7005 & -146 \\ 25 & -146 & 7060 \end{pmatrix}$	$\begin{pmatrix} 7105 \\ 6863 \\ 7189 \end{pmatrix}$	$\begin{pmatrix} 0.91 & 0.03 & 0.41 \\ -0.29 & 0.75 & 0.59 \\ -0.29 & -0.66 & 0.69 \end{pmatrix}$
	$1^5D_{3^{++}(3\bar{3})_c(\xi_3)}$		6863	
$1^5D_{3^{++}(6\bar{6})_c(\xi_1\xi_2)}$		7189		
4^{+-}	$1^5D_{4^{+-}(3\bar{3})_c(\xi_1\xi_2)}$	(7122)	7122	1
	$1^5D_{4^{++}(3\bar{3})_c(\xi_1\xi_2)}$	$\begin{pmatrix} 7108 & 72 & 31 \\ 72 & 7020 & -153 \\ 31 & -153 & 7079 \end{pmatrix}$	$\begin{pmatrix} 7126 \\ 6870 \\ 7211 \end{pmatrix}$	$\begin{pmatrix} 0.92 & 0.07 & 0.39 \\ -0.3 & 0.75 & 0.59 \\ 0.25 & 0.66 & -0.71 \end{pmatrix}$
4^{++}	$1^5D_{4^{++}(3\bar{3})_c(\xi_1\xi_2)}$		7126	
	$1^5D_{4^{++}(3\bar{3})_c(\xi_3)}$		6870	
	$1^5D_{4^{++}(6\bar{6})_c(\xi_1\xi_2)}$		7211	

- (2021).
- [34] H. Mutuk, Nonrelativistic treatment of fully-heavy tetraquarks as diquark-antidiquark states, *Eur. Phys. J. C* **81**, 367 (2021).
- [35] G. Yang, J. Ping and J. Segovia, Exotic resonances of fully-heavy tetraquarks in a lattice-QCD inspired quark model, *Phys. Rev. D* **104**, 014006 (2021).
- [36] R. N. Faustov, V. O. Galkin and E. M. Savchenko, Heavy tetraquarks in the relativistic quark model, *Universe* **7**, 94 (2021).
- [37] R. N. Faustov, V. O. Galkin and E. M. Savchenko, Masses of the $QQ\bar{Q}\bar{Q}$ tetraquarks in the relativistic diquark-antidiquark picture, *Phys. Rev. D* **102**, 114030 (2020).
- [38] M. C. Gordillo, F. De Soto and J. Segovia, Diffusion Monte Carlo calculations of fully-heavy multi-quark bound states, *Phys. Rev. D* **102**, 114007 (2020).
- [39] Z. Zhao, K. Xu, A. Kaewnsod, X. Liu, A. Limphirat and Y. Yan, Study of charmonium-like and fully-charm tetraquark spectroscopy, *Phys. Rev. D* **103**, 116027 (2021).
- [40] J. Zhao, S. Shi and P. Zhuang, Fully-heavy tetraquarks in a strongly interacting medium, *Phys. Rev. D* **102**, 114001 (2020).
- [41] M. Karliner and J. L. Rosner, Interpretation of structure in the di- J/ψ spectrum, *Phys. Rev. D* **102**, 114039 (2020).
- [42] X. Jin, Y. Xue, H. Huang and J. Ping, Full-heavy tetraquarks in constituent quark models, *Eur. Phys. J. C* **80**, 1083 (2020).
- [43] J. R. Zhang, 0^+ fully-charmed tetraquark states, *Phys. Rev. D* **103**, 014018 (2021).
- [44] B. C. Yang, L. Tang and C. F. Qiao, Scalar fully-heavy tetraquark states $QQ'\bar{Q}\bar{Q}'$ in QCD sum rules, *Eur. Phys. J. C* **81**, 324 (2021).
- [45] G. Yang, J. Ping, L. He and Q. Wang, Potential model prediction of fully-heavy tetraquarks $QQ\bar{Q}\bar{Q}$ ($Q = c, b$), arXiv:2006.13756 [hep-ph].
- [46] Q. F. Lü, D. Y. Chen and Y. B. Dong, Masses of fully heavy tetraquarks $QQ\bar{Q}\bar{Q}$ in an extended relativized quark model, *Eur. Phys. J. C* **80**, 871 (2020).
- [47] Z. G. Wang, Tetraquark candidates in the LHCb's di- J/ψ mass spectrum, *Chin. Phys. C* **44**, 113106 (2020).
- [48] Z. G. Wang, Revisit the tetraquark candidates in the $J/\psi J/\psi$ mass spectrum, *Int. J. Mod. Phys. A* **36**, 2150014 (2021).
- [49] H. W. Ke, X. Han, X. H. Liu and Y. L. Shi, Tetraquark state $X(6900)$ and the interaction between diquark and antidiquark, *Eur. Phys. J. C* **81**, 427 (2021).
- [50] R. Zhu, Fully-heavy tetraquark spectra and production at hadron colliders, *Nucl. Phys. B* **966**, 115393 (2021).

TABLE IX: Predicted mass spectrum for the 1D-wave $T_{(bb\bar{b}\bar{b})}$ states.

J^{PC}	Configuration	$\langle H \rangle$ (MeV)	Mass (MeV)	Eigenvector
0^{+-}	$1^3P_{0^{+-}(\bar{66})_c}(\xi_1\xi_3, \xi_2\xi_3)$	$\begin{pmatrix} 19693 & -116 \\ -116 & 19775 \end{pmatrix}$	$\begin{pmatrix} 19611 \\ 19857 \end{pmatrix}$	$\begin{pmatrix} -0.82 & -0.58 \\ 0.58 & -0.82 \end{pmatrix}$
	$1^3P_{0^{+-}(\bar{33})_c}(\xi_1\xi_3, \xi_2\xi_3)$			
	$1^5D_{0^{+-}(\bar{33})_c}(\xi_1, \xi_2)$	(19884)	19884	1
0^{++}	$1^1S_{0^{++}(\bar{33})_c}(\xi_1\xi_2)$	(19677)	19677	1
	$1^1S_{0^{++}(\bar{66})_c}(\xi_1\xi_2)$	(19796)	19796	1
	$1^3P_{0^{++}(\bar{66})_c}(\xi_1\xi_3, \xi_2\xi_3)$	$\begin{pmatrix} 19688 & 125 \\ 125 & 19773 \end{pmatrix}$	$\begin{pmatrix} 19598 \\ 19863 \end{pmatrix}$	$\begin{pmatrix} -0.81 & 0.58 \\ 0.58 & 0.81 \end{pmatrix}$
	$1^3P_{0^{++}(\bar{33})_c}(\xi_1\xi_3, \xi_2\xi_3)$			
	$1^3P_{0^{++}(\bar{66})_c}(\xi_1\xi_2)$	(19884)	19884	1
	$1^5D_{0^{++}(\bar{33})_c}(\xi_1, \xi_2)$	$\begin{pmatrix} 19873 & 59 & 22 \\ 59 & 19800 & -126 \\ 22 & -126 & 19847 \end{pmatrix}$	$\begin{pmatrix} 19885 \\ 19677 \\ 19958 \end{pmatrix}$	$\begin{pmatrix} 0.91 & 0.04 & 0.4 \\ -0.29 & 0.75 & 0.59 \\ 0.28 & 0.66 & -0.7 \end{pmatrix}$
	$1^5D_{0^{++}(\bar{33})_c}(\xi_3)$			
1^{+-}	$1^3S_{1^{+-}(\bar{66})_c}(\xi_1\xi_3, \xi_2\xi_3)$	$\begin{pmatrix} 19812 & -24 \\ -24 & 19828 \end{pmatrix}$	$\begin{pmatrix} 19795 \\ 19845 \end{pmatrix}$	$\begin{pmatrix} 0.81 & 0.58 \\ 0.58 & -0.81 \end{pmatrix}$
	$1^3S_{1^{+-}(\bar{33})_c}(\xi_1\xi_3, \xi_2\xi_3)$			
	$1^3S_{1^{+-}(\bar{66})_c}(\xi_1\xi_2)$	(19802)	19802	1
	$1^1P_{1^{+-}(\bar{33})_c}(\xi_1\xi_2)$	(19711)	19711	1
	$1^1P_{1^{+-}(\bar{66})_c}(\xi_1\xi_2)$	(19883)	19883	1
	$1^3P_{1^{+-}(\bar{66})_c}(\xi_1\xi_3, \xi_2\xi_3)$	$\begin{pmatrix} 19692 & -116 \\ -116 & 19774 \end{pmatrix}$	$\begin{pmatrix} 19610 \\ 19856 \end{pmatrix}$	$\begin{pmatrix} -0.82 & -0.58 \\ -0.58 & 0.82 \end{pmatrix}$
	$1^3P_{1^{+-}(\bar{33})_c}(\xi_1\xi_3, \xi_2\xi_3)$			
	$1^5P_{1^{+-}(\bar{66})_c}(\xi_1\xi_2)$	(19890)	19890	1
	$1^3D_{1^{+-}(\bar{33})_c}(\xi_1, \xi_2)$	$\begin{pmatrix} 19877 & 62 & 26 \\ 62 & 19803 & -131 \\ 26 & -131 & 19845 \end{pmatrix}$	$\begin{pmatrix} 19671 \\ 19891 \\ 19963 \end{pmatrix}$	$\begin{pmatrix} -0.30 & 0.74 & 0.60 \\ 0.91 & 0.04 & 0.41 \\ 0.28 & 0.67 & -0.69 \end{pmatrix}$
	$1^3D_{1^{+-}(\bar{33})_c}(\xi_3)$			
	$1^3D_{1^{+-}(\bar{66})_c}(\xi_1\xi_2)$			
	$1^3D_{1^{+-}(\bar{66})_c}(\xi_1\xi_3, \xi_2\xi_3)$	$\begin{pmatrix} 19906 & 70 \\ 70 & 19856 \end{pmatrix}$	$\begin{pmatrix} 19955 \\ 19807 \end{pmatrix}$	$\begin{pmatrix} -0.82 & -0.58 \\ 0.58 & -0.82 \end{pmatrix}$
	$1^3D_{1^{+-}(\bar{33})_c}(\xi_1\xi_3, \xi_2\xi_3)$			
$1^5D_{1^{+-}(\bar{33})_c}(\xi_1, \xi_2)$	(19887)	19887	1	
1^{++}	$1^3S_{1^{++}(\bar{66})_c}(\xi_1\xi_3, \xi_2\xi_3)$	$\begin{pmatrix} 19807 & 34 \\ 34 & 19827 \end{pmatrix}$	$\begin{pmatrix} 19782 \\ 19852 \end{pmatrix}$	$\begin{pmatrix} -0.8 & 0.6 \\ 0.6 & 0.8 \end{pmatrix}$
	$1^3S_{1^{++}(\bar{33})_c}(\xi_1\xi_3, \xi_2\xi_3)$			
	$1^3P_{1^{++}(\bar{66})_c}(\xi_1\xi_3, \xi_2\xi_3)$	$\begin{pmatrix} 19690 & 127 \\ 127 & 19773 \end{pmatrix}$	$\begin{pmatrix} 19598 \\ 19865 \end{pmatrix}$	$\begin{pmatrix} -0.81 & 0.59 \\ 0.59 & 0.81 \end{pmatrix}$
	$1^3P_{1^{++}(\bar{33})_c}(\xi_1\xi_3, \xi_2\xi_3)$			
	$1^3P_{1^{++}(\bar{66})_c}(\xi_1\xi_2)$	(19883)	19883	1
	$1^3D_{1^{++}(\bar{33})_c}(\xi_1, \xi_2)$	(19889)	19889	1
	$1^3D_{1^{++}(\bar{66})_c}(\xi_1\xi_3, \xi_2\xi_3)$	$\begin{pmatrix} 19907 & -62 \\ -62 & 19856 \end{pmatrix}$	$\begin{pmatrix} 19949 \\ 19814 \end{pmatrix}$	$\begin{pmatrix} -0.83 & 0.55 \\ 0.56 & 0.83 \end{pmatrix}$
	$1^3D_{1^{++}(\bar{33})_c}(\xi_1\xi_3, \xi_2\xi_3)$			
	$1^5D_{1^{++}(\bar{33})_c}(\xi_1, \xi_2)$	$\begin{pmatrix} 19876 & 60 & 23 \\ 60 & 19802 & -127 \\ 23 & -127 & 19850 \end{pmatrix}$	$\begin{pmatrix} 19889 \\ 19678 \\ 19961 \end{pmatrix}$	$\begin{pmatrix} 0.91 & 0.04 & 0.4 \\ -0.3 & 0.75 & 0.59 \\ 0.28 & 0.66 & -0.7 \end{pmatrix}$
	$1^5D_{1^{++}(\bar{33})_c}(\xi_3)$			
$1^5D_{1^{++}(\bar{66})_c}(\xi_1\xi_2)$				
2^{+-}	$1^3P_{2^{+-}(\bar{66})_c}(\xi_1\xi_3, \xi_2\xi_3)$	$\begin{pmatrix} 19695 & -119 \\ -119 & 19779 \end{pmatrix}$	$\begin{pmatrix} 19611 \\ 19863 \end{pmatrix}$	$\begin{pmatrix} -0.82 & -0.58 \\ -0.58 & 0.82 \end{pmatrix}$
	$1^3P_{2^{+-}(\bar{33})_c}(\xi_1\xi_3, \xi_2\xi_3)$			
	$1^5P_{2^{+-}(\bar{66})_c}(\xi_1\xi_2)$	(19891)	19891	1
	$1^1D_{2^{+-}(\bar{66})_c}(\xi_1, \xi_2)$	(19807)	19807	1
	$1^1D_{2^{+-}(\bar{33})_c}(\xi_1, \xi_2)$	(19895)	19895	1
	$1^3D_{2^{+-}(\bar{33})_c}(\xi_1, \xi_2)$	$\begin{pmatrix} 19881 & 63 & 29 \\ 63 & 19806 & -133 \\ 29 & -133 & 19852 \end{pmatrix}$	$\begin{pmatrix} 19672 \\ 19898 \\ 19969 \end{pmatrix}$	$\begin{pmatrix} -0.31 & 0.74 & 0.60 \\ 0.92 & 0.07 & 0.39 \\ 0.25 & 0.67 & -0.70 \end{pmatrix}$
	$1^3D_{2^{+-}(\bar{33})_c}(\xi_3)$			
	$1^3D_{2^{+-}(\bar{66})_c}(\xi_1\xi_2)$			
	$1^3D_{2^{+-}(\bar{66})_c}(\xi_1\xi_3, \xi_2\xi_3)$	$\begin{pmatrix} 19910 & 68 \\ 68 & 19863 \end{pmatrix}$	$\begin{pmatrix} 19958 \\ 19815 \end{pmatrix}$	$\begin{pmatrix} -0.81 & -0.58 \\ 0.58 & -0.81 \end{pmatrix}$
	$1^3D_{2^{+-}(\bar{33})_c}(\xi_1\xi_3, \xi_2\xi_3)$			
$1^5D_{2^{+-}(\bar{33})_c}(\xi_1, \xi_2)$	(19893)	19893	1	

- [51] G. J. Wang, L. Meng, M. Oka and S. L. Zhu, Higher fully-charmed tetraquarks: radial excitations and P-wave states, Phys. Rev. D **104**, 036016 (2021).
- [52] J. F. Giron and R. F. Lebed, Simple spectrum of $c\bar{c}c\bar{c}$ states in the dynamical diquark model, Phys. Rev. D **102**, 074003 (2020).
- [53] A. J. Majarshin, Y. A. Luo, F. Pan and J. Segovia, The bosonic

algebraic approach applied to the $[QQ][\bar{Q}\bar{Q}]$ tetraquarks, arXiv:2106.01179 [hep-ph].

- [54] X. Z. Weng, X. L. Chen, W. Z. Deng and S. L. Zhu, Systematics of fully heavy tetraquarks, Phys. Rev. D **103**, 034001 (2021).
- [55] J. Sonnenschein and D. Weissman, Deciphering the recently discovered tetraquark candidates around 6.9 GeV, Eur. Phys. J. C **81**, 25 (2021).

TABLE X: Predicted mass spectrum for the $1D$ -wave $T_{(bb\bar{b}\bar{b})}$ states (Continued).

J^{PC}	Configuration	$\langle H \rangle$ (MeV)	Mass (MeV)	Eigenvector
	$1^5S_{2^{++}(6\bar{6})_c(\xi_1\xi_2)}$	(19814)	19814	1
	$1^3P_{2^{++}(6\bar{6})_c(\xi_1\xi_3\xi_2\xi_3)}$	$\begin{pmatrix} 19691 & 129 \\ 129 & 19777 \end{pmatrix}$	$\begin{pmatrix} 19598 \\ 19870 \end{pmatrix}$	$\begin{pmatrix} -0.81 & 0.58 \\ 0.58 & 0.81 \end{pmatrix}$
2^{++}	$1^3P_{2^{++}(3\bar{3})_c(\xi_1\xi_3\xi_2\xi_3)}$	(19891)	19891	1
	$1^3P_{2^{++}(6\bar{6})_c(\xi_1\xi_2)}$	(19891)	19891	1
	$1^1D_{2^{++}(6\bar{6})_c(\xi_1\xi_2)}$	$\begin{pmatrix} 19773 & 156 & 29 \\ 156 & 19770 & -133 \\ 29 & -133 & 19697 \end{pmatrix}$	$\begin{pmatrix} 19952 \\ 19758 \\ 19530 \end{pmatrix}$	$\begin{pmatrix} -0.59 & -0.74 & 0.32 \\ 0.64 & -0.2 & 0.74 \\ 0.48 & -0.64 & -0.59 \end{pmatrix}$
	$1^1D_{2^{++}(6\bar{6})_c(\xi_3)}$	$\begin{pmatrix} 19881 & 63 & 30 \\ 63 & 19806 & -135 \\ 30 & -135 & 19848 \end{pmatrix}$	$\begin{pmatrix} 19968 \\ 19669 \\ 19898 \end{pmatrix}$	$\begin{pmatrix} 0.25 & 0.67 & -0.7 \\ -0.3 & 0.74 & 0.61 \\ 0.92 & 0.06 & 0.39 \end{pmatrix}$
	$1^1D_{2^{++}(3\bar{3})_c(\xi_1\otimes\xi_2)}$	$\begin{pmatrix} 19881 & 61 & 26 \\ 61 & 19807 & -129 \\ 26 & -129 & 19856 \end{pmatrix}$	$\begin{pmatrix} 19896 \\ 19680 \\ 19968 \end{pmatrix}$	$\begin{pmatrix} 0.92 & 0.06 & 0.39 \\ -0.3 & 0.75 & 0.59 \\ 0.25 & 0.66 & -0.7 \end{pmatrix}$
	$1^1D_{2^{++}(3\bar{3})_c(\xi_3)}$	$\begin{pmatrix} 19881 & 61 & 26 \\ 61 & 19807 & -129 \\ 26 & -129 & 19856 \end{pmatrix}$	$\begin{pmatrix} 19896 \\ 19680 \\ 19968 \end{pmatrix}$	$\begin{pmatrix} 0.92 & 0.06 & 0.39 \\ -0.3 & 0.75 & 0.59 \\ 0.25 & 0.66 & -0.7 \end{pmatrix}$
	$1^1D_{2^{++}(6\bar{6})_c(\xi_1\otimes\xi_2)}$	(19894)	19894	1
	$1^3D_{2^{++}(3\bar{3})_c(\xi_1\xi_2)}$	(19894)	19894	1
	$1^3D_{2^{++}(6\bar{6})_c(\xi_1\xi_3\xi_2\xi_3)}$	$\begin{pmatrix} 19910 & -63 \\ -63 & 19862 \end{pmatrix}$	$\begin{pmatrix} 19953 \\ 19819 \end{pmatrix}$	$\begin{pmatrix} -0.82 & 0.57 \\ -0.57 & -0.82 \end{pmatrix}$
	$1^3D_{2^{++}(3\bar{3})_c(\xi_1\xi_3\xi_2\xi_3)}$	$\begin{pmatrix} 19910 & -63 \\ -63 & 19862 \end{pmatrix}$	$\begin{pmatrix} 19953 \\ 19819 \end{pmatrix}$	$\begin{pmatrix} -0.82 & 0.57 \\ -0.57 & -0.82 \end{pmatrix}$
	$1^5D_{2^{++}(3\bar{3})_c(\xi_1\xi_2)}$	$\begin{pmatrix} 19881 & 61 & 26 \\ 61 & 19807 & -129 \\ 26 & -129 & 19856 \end{pmatrix}$	$\begin{pmatrix} 19896 \\ 19680 \\ 19968 \end{pmatrix}$	$\begin{pmatrix} 0.92 & 0.06 & 0.39 \\ -0.3 & 0.75 & 0.59 \\ 0.25 & 0.66 & -0.7 \end{pmatrix}$
	$1^5D_{2^{++}(3\bar{3})_c(\xi_3)}$	$\begin{pmatrix} 19881 & 61 & 26 \\ 61 & 19807 & -129 \\ 26 & -129 & 19856 \end{pmatrix}$	$\begin{pmatrix} 19896 \\ 19680 \\ 19968 \end{pmatrix}$	$\begin{pmatrix} 0.92 & 0.06 & 0.39 \\ -0.3 & 0.75 & 0.59 \\ 0.25 & 0.66 & -0.7 \end{pmatrix}$
	$1^5D_{2^{++}(6\bar{6})_c(\xi_1\xi_2)}$	$\begin{pmatrix} 19881 & 61 & 26 \\ 61 & 19807 & -129 \\ 26 & -129 & 19856 \end{pmatrix}$	$\begin{pmatrix} 19896 \\ 19680 \\ 19968 \end{pmatrix}$	$\begin{pmatrix} 0.92 & 0.06 & 0.39 \\ -0.3 & 0.75 & 0.59 \\ 0.25 & 0.66 & -0.7 \end{pmatrix}$
3^{+-}	$1^5P_{3^{+-}(6\bar{6})_c(\xi_1\xi_2)}$	(19902)	19902	1
	$1^3D_{3^{+-}(3\bar{3})_c(\xi_1\xi_2)}$	$\begin{pmatrix} 19887 & 64 & 31 \\ 64 & 19812 & -135 \\ 31 & -135 & 19857 \end{pmatrix}$	$\begin{pmatrix} 19675 \\ 19905 \\ 19976 \end{pmatrix}$	$\begin{pmatrix} -0.31 & 0.74 & 0.60 \\ 0.92 & 0.07 & 0.39 \\ 0.24 & 0.67 & -0.70 \end{pmatrix}$
	$1^3D_{3^{+-}(3\bar{3})_c(\xi_3)}$	$\begin{pmatrix} 19887 & 64 & 31 \\ 64 & 19812 & -135 \\ 31 & -135 & 19857 \end{pmatrix}$	$\begin{pmatrix} 19675 \\ 19905 \\ 19976 \end{pmatrix}$	$\begin{pmatrix} -0.31 & 0.74 & 0.60 \\ 0.92 & 0.07 & 0.39 \\ 0.24 & 0.67 & -0.70 \end{pmatrix}$
	$1^3D_{3^{+-}(6\bar{6})_c(\xi_1\xi_2)}$	$\begin{pmatrix} 19917 & 68 \\ 68 & 19869 \end{pmatrix}$	$\begin{pmatrix} 19965 \\ 19821 \end{pmatrix}$	$\begin{pmatrix} -0.82 & -0.58 \\ 0.58 & -0.82 \end{pmatrix}$
	$1^3D_{3^{+-}(6\bar{6})_c(\xi_1\xi_3\xi_2\xi_3)}$	$\begin{pmatrix} 19917 & 68 \\ 68 & 19869 \end{pmatrix}$	$\begin{pmatrix} 19965 \\ 19821 \end{pmatrix}$	$\begin{pmatrix} -0.82 & -0.58 \\ 0.58 & -0.82 \end{pmatrix}$
	$1^3D_{3^{+-}(3\bar{3})_c(\xi_1\xi_3\xi_2\xi_3)}$	$\begin{pmatrix} 19917 & 68 \\ 68 & 19869 \end{pmatrix}$	$\begin{pmatrix} 19965 \\ 19821 \end{pmatrix}$	$\begin{pmatrix} -0.82 & -0.58 \\ 0.58 & -0.82 \end{pmatrix}$
	$1^5D_{3^{+-}(3\bar{3})_c(\xi_1\xi_2)}$	(19901)	19901	1
3^{++}	$1^3D_{3^{++}(3\bar{3})_c(\xi_1\xi_2)}$	(19901)	19901	1
	$1^3D_{3^{++}(6\bar{6})_c(\xi_1\xi_3\xi_2\xi_3)}$	$\begin{pmatrix} 19917 & -61 \\ -61 & 19869 \end{pmatrix}$	$\begin{pmatrix} 19959 \\ 19827 \end{pmatrix}$	$\begin{pmatrix} 0.83 & -0.56 \\ 0.56 & 0.83 \end{pmatrix}$
	$1^3D_{3^{++}(3\bar{3})_c(\xi_1\xi_3\xi_2\xi_3)}$	$\begin{pmatrix} 19917 & -61 \\ -61 & 19869 \end{pmatrix}$	$\begin{pmatrix} 19959 \\ 19827 \end{pmatrix}$	$\begin{pmatrix} 0.83 & -0.56 \\ 0.56 & 0.83 \end{pmatrix}$
	$1^5D_{3^{++}(3\bar{3})_c(\xi_1\xi_2)}$	$\begin{pmatrix} 19887 & 62 & 28 \\ 62 & 19813 & -131 \\ 28 & -131 & 19864 \end{pmatrix}$	$\begin{pmatrix} 19904 \\ 19684 \\ 19976 \end{pmatrix}$	$\begin{pmatrix} 0.92 & 0.08 & 0.38 \\ -0.31 & 0.75 & 0.59 \\ -0.24 & -0.66 & 0.71 \end{pmatrix}$
	$1^5D_{3^{++}(3\bar{3})_c(\xi_3)}$	$\begin{pmatrix} 19887 & 62 & 28 \\ 62 & 19813 & -131 \\ 28 & -131 & 19864 \end{pmatrix}$	$\begin{pmatrix} 19904 \\ 19684 \\ 19976 \end{pmatrix}$	$\begin{pmatrix} 0.92 & 0.08 & 0.38 \\ -0.31 & 0.75 & 0.59 \\ -0.24 & -0.66 & 0.71 \end{pmatrix}$
	$1^5D_{3^{++}(6\bar{6})_c(\xi_1\xi_2)}$	$\begin{pmatrix} 19887 & 62 & 28 \\ 62 & 19813 & -131 \\ 28 & -131 & 19864 \end{pmatrix}$	$\begin{pmatrix} 19904 \\ 19684 \\ 19976 \end{pmatrix}$	$\begin{pmatrix} 0.92 & 0.08 & 0.38 \\ -0.31 & 0.75 & 0.59 \\ -0.24 & -0.66 & 0.71 \end{pmatrix}$
4^{+-}	$1^5D_{4^{+-}(3\bar{3})_c(\xi_1\xi_2)}$	(7122)	19908	1
4^{++}	$1^5D_{4^{++}(3\bar{3})_c(\xi_1\xi_2)}$	$\begin{pmatrix} 19894 & 63 & 30 \\ 63 & 19819 & -134 \\ 30 & -134 & 19871 \end{pmatrix}$	$\begin{pmatrix} 19912 \\ 19686 \\ 19985 \end{pmatrix}$	$\begin{pmatrix} 0.92 & 0.1 & 0.37 \\ -0.31 & 0.74 & 0.59 \\ -0.22 & -0.66 & 0.72 \end{pmatrix}$
	$1^5D_{4^{++}(3\bar{3})_c(\xi_3)}$	$\begin{pmatrix} 19894 & 63 & 30 \\ 63 & 19819 & -134 \\ 30 & -134 & 19871 \end{pmatrix}$	$\begin{pmatrix} 19912 \\ 19686 \\ 19985 \end{pmatrix}$	$\begin{pmatrix} 0.92 & 0.1 & 0.37 \\ -0.31 & 0.74 & 0.59 \\ -0.22 & -0.66 & 0.72 \end{pmatrix}$
	$1^5D_{4^{++}(6\bar{6})_c(\xi_1\xi_2)}$	$\begin{pmatrix} 19894 & 63 & 30 \\ 63 & 19819 & -134 \\ 30 & -134 & 19871 \end{pmatrix}$	$\begin{pmatrix} 19912 \\ 19686 \\ 19985 \end{pmatrix}$	$\begin{pmatrix} 0.92 & 0.1 & 0.37 \\ -0.31 & 0.74 & 0.59 \\ -0.22 & -0.66 & 0.72 \end{pmatrix}$

- [56] Y. Huang, F. Feng, Y. Jia, W. L. Sang, D. S. Yang and J. Y. Zhang, Inclusive production of fully-charmed 1^{+-} tetraquark at B factory, Chin. Phys. C **45**, 093101 (2021).
- [57] X. Y. Wang, Q. Y. Lin, H. Xu, Y. P. Xie, Y. Huang and X. Chen, Discovery potential for the LHCb fully-charm tetraquark $X(6900)$ state via $\bar{p}p$ annihilation reaction, Phys. Rev. D **102**, 116014 (2020).
- [58] V. P. Goncalves and B. D. Moreira, Fully - heavy tetraquark production by $\gamma\gamma$ interactions in hadronic collisions at the LHC, Phys. Lett. B **816**, 136249 (2021).
- [59] F. Feng, Y. Huang, Y. Jia, W. L. Sang and J. Y. Zhang, Exclusive radiative production of fully-charmed tetraquarks at B Factory, Phys. Lett. B **818**, 136368 (2021).
- [60] F. Feng, Y. Huang, Y. Jia, W. L. Sang, X. Xiong and J. Y. Zhang, Fragmentation production of fully-charmed tetraquarks at LHC, arXiv:2009.08450 [hep-ph].
- [61] Y. Q. Ma and H. F. Zhang, Exploring the Di- J/ψ Resonances around 6.9 GeV Based on ab *initio* Perturbative QCD, arXiv:2009.08376 [hep-ph].
- [62] R. Maciula, W. Schäfer and A. Szczurek, On the mechanism of $T_{4c}(6900)$ tetraquark production, Phys. Lett. B **812**, 136010 (2021).
- [63] H. X. Chen, W. Chen, X. Liu and S. L. Zhu, Strong decays of fully-charm tetraquarks into di-charmonia, Sci. Bull. **65**, 1994 (2020).
- [64] C. Becchi, J. Ferretti, A. Giachino, L. Maiani and E. Santopinto, A study of $cc\bar{c}\bar{c}$ tetraquark decays in 4 muons and in $D^{(*)}\bar{D}^{(*)}$ at LHC, Phys. Lett. B **811**, 135952 (2020).
- [65] Z. R. Liang, X. Y. Wu and D. L. Yao, Hunting for states in the recent LHCb di- J/ψ invariant mass spectrum, Phys. Rev. D **104**, 034034 (2021).
- [66] X. K. Dong, F. K. Guo and B. S. Zou, Explaining the Many Threshold Structures in the Heavy-Quark Hadron Spectrum, Phys. Rev. Lett. **126**, 152001 (2021).
- [67] X. K. Dong, V. Baru, F. K. Guo, C. Hanhart and A. Nefediev, Coupled-Channel Interpretation of the LHCb Double- J/ψ Spectrum and Hints of a New State Near the $J/\psi J/\psi$ Threshold, Phys. Rev. Lett. **126**, 132001 (2021).
- [68] J. Z. Wang, D. Y. Chen, X. Liu and T. Matsuki, Producing fully charm structures in the J/ψ -pair invariant mass spectrum, Phys. Rev. D **103**, 071503 (2021).
- [69] Z. H. Guo and J. A. Oller, Insights into the inner structures of the fully charmed tetraquark state $X(6900)$, Phys. Rev. D **103**, 034024 (2021).

TABLE XI: The average contributions of each part of the Hamiltonian to the $2S$ - and $3S$ -wave $T_{(ccc\bar{c})}$ configurations. $\langle T \rangle$ stands for the contribution of the kinetic energy term. $\langle V^{Lin} \rangle$ and $\langle V^{Coul} \rangle$ stand for the contributions from the linear confinement potential and Coulomb type potential, respectively. $\langle V^{SS} \rangle$, $\langle V^T \rangle$, and $\langle V^{LS} \rangle$ stand for the contributions from the spin-spin interaction term, the tensor potential term, and the spin-orbit interaction term, respectively.

J^{PC}	Configuration	Mass	$\langle T \rangle$	$\langle V^{Lin} \rangle$	$\langle V^{Coul} \rangle$	$\langle V^{SS} \rangle$
0^{+-}	$2^1S_{0^{+-}(\bar{6}\bar{6})_c(\xi_1, \xi_2)}$	7008	706	899	-540	10.18
	$2^1S_{0^{+-}(\bar{3}\bar{3})_c(\xi_1, \xi_2)}$	7005	776	924	-629	2.75
0^{++}	$2^1S_{0^{++}(\bar{6}\bar{6})_c(\xi_1, \xi_2)}$	6954	725	883	-598	11.39
	$2^1S_{0^{++}(\bar{3}\bar{3})_c(\xi_1, \xi_2)}$	7000	774	919	-622	-3.79
	$2^1S_{0^{++}(\bar{6}\bar{6})_c(\xi_3)}$	7183	757	1010	-522	6.52
	$2^1S_{0^{++}(\bar{3}\bar{3})_c(\xi_3)}$	6930	761	876	-642	2.56
1^{+-}	$2^3S_{1^{+-}(\bar{3}\bar{3})_c(\xi_1, \xi_2)}$	7006	774	920	-622	2.32
	$2^3S_{1^{+-}(\bar{3}\bar{3})_c(\xi_3)}$	6934	745	885	-634	6.18
1^{++}	$2^3S_{1^{++}(\bar{3}\bar{3})_c(\xi_1, \xi_2)}$	7009	773	925	-628	6.88
2^{+-}	$2^5S_{2^{+-}(\bar{3}\bar{3})_c(\xi_1, \xi_2)}$	7017	762	932	-624	14.99
2^{++}	$2^5S_{2^{++}(\bar{3}\bar{3})_c(\xi_1, \xi_2)}$	7018	753	932	-613	13.94
	$2^5S_{2^{++}(\bar{3}\bar{3})_c(\xi_3)}$	6942	741	888	-633	13.96
0^{+-}	$3^1S_{0^{+-}(\bar{6}\bar{6})_c(\xi_1, \xi_2)}$	7356	761	1103	-449	8.75
	$3^1S_{0^{+-}(\bar{3}\bar{3})_c(\xi_1, \xi_2)}$	7396	839	1151	-528	1.9
0^{++}	$3^1S_{0^{++}(\bar{6}\bar{6})_c(\xi_1, \xi_2)}$	7347	764	1097	-455	9.02
	$3^1S_{0^{++}(\bar{3}\bar{3})_c(\xi_1, \xi_2)}$	7403	838	1150	-518	0.53
	$3^1S_{0^{++}(\bar{6}\bar{6})_c(\xi_3)}$	7720	855	1326	-397	4.59
	$3^1S_{0^{++}(\bar{3}\bar{3})_c(\xi_3)}$	7241	815	1064	-575	4.46
1^{+-}	$3^3S_{1^{+-}(\bar{3}\bar{3})_c(\xi_1, \xi_2)}$	7406	828	1157	-515	3.6
	$3^3S_{1^{+-}(\bar{3}\bar{3})_c(\xi_3)}$	7243	814	1065	-575	7.06
1^{++}	$3^3S_{1^{++}(\bar{3}\bar{3})_c(\xi_1, \xi_2)}$	7399	838	1152	-528	4.88
2^{+-}	$3^5S_{2^{+-}(\bar{3}\bar{3})_c(\xi_1, \xi_2)}$	7405	835	1154	-527	10.81
2^{++}	$3^5S_{2^{++}(\bar{3}\bar{3})_c(\xi_1, \xi_2)}$	7412	825	1160	-514	9.67
	$3^5S_{2^{++}(\bar{3}\bar{3})_c(\xi_3)}$	7248	812	1067	-575	12.3

- [70] C. Gong, M. C. Du, Q. Zhao, X. H. Zhong and B. Zhou, Nature of $X(6900)$ and its production mechanism at LHCb, Phys. Lett. B **824**, 136794 (2022).
- [71] Q. F. Cao, H. Chen, H. R. Qi and H. Q. Zheng, Some remarks on $X(6900)$, Chin. Phys. C **45**, 103102 (2021).
- [72] B. D. Wan and C. F. Qiao, Gluonic tetracharm configuration of $X(6900)$, Phys. Lett. B **817**, 136339 (2021).
- [73] J. W. Zhu, X. D. Guo, R. Y. Zhang, W. G. Ma and X. Q. Li, A possible interpretation for $X(6900)$ observed in four-muon final state by LHCb—A light Higgs-like boson?, arXiv:2011.07799 [hep-ph].
- [74] M. Z. Liu and L. S. Geng, Is $X(7200)$ the heavy anti-quark di-quark symmetry partner of $X(3872)$?, Eur. Phys. J. C **81**, 179 (2021).
- [75] E. Eichten, K. Gottfried, T. Kinoshita, K. D. Lane and T. M. Yan, Charmonium: The model, Phys. Rev. D **17**, 3090 (1978); **21**, 313(E) (1980).
- [76] F. X. Liu, M. S. Liu, X. H. Zhong and Q. Zhao, Fully-strange tetraquark $ss\bar{s}\bar{s}$ spectrum and possible experimental evidence, Phys. Rev. D **103**, 016016 (2021).
- [77] E. Hiyama, Y. Kino and M. Kamimura, Gaussian expansion method for few-body systems, Prog. Part. Nucl. Phys. **51**, 223 (2003).
- [78] E. Hiyama and M. Kamimura, Study of various few-body systems using Gaussian expansion method (GEM), Front. Phys. (Beijing) **13**, 132106 (2018).
- [79] S. Godfrey and N. Isgur, Mesons in a relativized quark model with chromodynamics, Phys. Rev. D **32**, 189 (1985).
- [80] T. Barnes, S. Godfrey, and E. S. Swanson, Higher charmonia, Phys. Rev. D **72**, 054026 (2005).
- [81] S. Godfrey, Spectroscopy of B_c mesons in the relativized quark model, Phys. Rev. D **70**, 054017 (2004).
- [82] S. Godfrey and K. Moats, Bottomonium mesons and strategies for their observation, Phys. Rev. D **92**, 054034 (2015).
- [83] O. Lakhina and E. S. Swanson, A canonical $D_s(2317)$, Phys. Lett. B **650**, 159 (2007)

TABLE XII: The average contributions of each part of the Hamiltonian to the $2S$ - and $3S$ -wave $T_{(bb\bar{b}\bar{b})}$ configurations.

J^{PC}	Configuration	Mass	$\langle T \rangle$	$\langle V^{Lin} \rangle$	$\langle V^{Coul} \rangle$	$\langle V^{SS} \rangle$
0^{+-}	$2^1S_{0^{+-}(6\bar{6})_c(\xi_1, \xi_2)}$	19840	627	529	-727	3.99
	$2^1S_{0^{+-}(\bar{3}3)_c(\xi_1, \xi_2)}$	19790	701	543	-864	2.28
0^{++}	$2^1S_{0^{++}(6\bar{6})_c(\xi_1, \xi_2)}$	19770	653	515	-810	4.48
	$2^1S_{0^{++}(\bar{3}3)_c(\xi_1, \xi_2)}$	19797	690	538	-837	-1.21
	$2^1S_{0^{++}(6\bar{6})_c(\xi_3)}$	19972	646	604	-688	2.36
	$2^1S_{0^{++}(\bar{3}3)_c(\xi_3)}$	19733	694	510	-881	1.58
1^{+-}	$2^3S_{1^{+-}(\bar{3}3)_c(\xi_1, \xi_2)}$	19800	690	538	-837	1.14
	$2^3S_{1^{+-}(\bar{3}3)_c(\xi_3)}$	19735	693	511	-880	3.09
1^{++}	$2^3S_{1^{++}(\bar{3}3)_c(\xi_1, \xi_2)}$	19792	700	543	-863	3.81
2^{+-}	$2^5S_{2^{+-}(\bar{3}3)_c(\xi_1, \xi_2)}$	19795	692	546	-859	6.83
2^{++}	$2^5S_{2^{++}(\bar{3}3)_c(\xi_1, \xi_2)}$	19804	671	545	-826	5.60
	$2^5S_{2^{++}(\bar{3}3)_c(\xi_3)}$	19738	692	512	-880	6.11
0^{+-}	$3^1S_{0^{+-}(6\bar{6})_c(\xi_1, \xi_2)}$	20128	622	675	-580	3.07
	$3^1S_{0^{+-}(\bar{3}3)_c(\xi_1, \xi_2)}$	20115	696	701	-691	1.26
0^{++}	$3^1S_{0^{++}(6\bar{6})_c(\xi_1, \xi_2)}$	20120	627	669	-587	3.19
	$3^1S_{0^{++}(\bar{3}3)_c(\xi_1, \xi_2)}$	20128	688	703	-671	0.49
	$3^1S_{0^{++}(6\bar{6})_c(\xi_3)}$	20405	661	833	-498	1.41
	$3^1S_{0^{++}(\bar{3}3)_c(\xi_3)}$	19979	710	640	-782	2.37
1^{+-}	$3^3S_{1^{+-}(\bar{3}3)_c(\xi_1, \xi_2)}$	20129	687	703	-670	1.54
	$3^3S_{1^{+-}(\bar{3}3)_c(\xi_3)}$	19980	710	641	-782	3.3
1^{++}	$3^3S_{1^{++}(\bar{3}3)_c(\xi_1, \xi_2)}$	20116	696	702	-691	2.27
2^{+-}	$3^5S_{2^{+-}(\bar{3}3)_c(\xi_1, \xi_2)}$	20118	695	702	-691	4.28
2^{++}	$3^5S_{2^{++}(\bar{3}3)_c(\xi_1, \xi_2)}$	20131	685	704	-670	3.64
	$3^5S_{2^{++}(\bar{3}3)_c(\xi_3)}$	19982	709	641	-782	5.19

- [84] Q. F. Lü, T. T. Pan, Y. Y. Wang, E. Wang and D. M. Li, Excited bottom and bottom-strange mesons in the quark model, Phys. Rev. D **94**, 074012 (2016).
- [85] D. M. Li, P. F. Ji, and B. Ma, The newly observed open-charm states in quark model, Eur. Phys. J. C **71**, 1582 (2011).
- [86] W. J. Deng, H. Liu, L. C. Gui, and X. H. Zhong, Charmonium spectrum and their electromagnetic transitions with higher multipole contributions, Phys. Rev. D **95**, 034026 (2017).
- [87] W. J. Deng, H. Liu, L. C. Gui, and X. H. Zhong, Spectrum and electromagnetic transitions of bottomonium, Phys. Rev. D **95**, 074002 (2017).
- [88] M. S. Liu, Q. F. Lü and X. H. Zhong, Triply charmed and bottom baryons in a constituent quark model, Phys. Rev. D **101**, 074031 (2020).
- [89] M. S. Liu, K. L. Wang, Q. F. Lü and X. H. Zhong, Ω baryon spectrum and their decays in a constituent quark model, Phys. Rev. D **101**, 016002 (2020).
- [90] Q. Li, L. C. Gui, M. S. Liu, Q. F. Lü and X. H. Zhong, Strangeonium meson spectrum in a constituent quark model, Chin. Phys. C **45**, 023116 (2021).
- [91] E. Hiyama, M. Kamimura, A. Hosaka, H. Toki and M. Yahiro, Five-body calculation of resonance and scattering states of pentaquark system, Phys. Lett. B **633**, 237 (2006).
- [92] E. Hiyama, A. Hosaka, M. Oka and J. M. Richard, Quark model estimate of hidden-charm pentaquark resonances, Phys. Rev. C **98**, 045208 (2018).
- [93] Q. Meng, E. Hiyama, K. U. Can, P. Gubler, M. Oka, A. Hosaka and H. Zong, Compact $sssc\bar{c}$ pentaquark states predicted by a quark model, Phys. Lett. B **798**, 135028 (2019).
- [94] Q. Meng, E. Hiyama, A. Hosaka, M. Oka, P. Gubler, K. U. Can, T. T. Takahashi and H. S. Zong, Stable double-heavy tetraquarks: spectrum and structure, Phys. Lett. B **814**, 136095 (2021).
- [95] K. Varga and Y. Suzuki, Stochastic variational method with a correlated Gaussian basis, Phys. Rev. A **53**, 1907 (1996).
- [96] K. Varga, Y. Ohbayasi and Y. Suzuki, Stochastic variational method with noncentral forces, Phys. Lett. B **396**, 1 (1997).
- [97] K. Varga and Y. Suzuki, Solution of few body problems with the stochastic variational method: 1. Central forces, Comput. Phys. Commun. **106**, 157 (1997).
- [98] D. M. Brink and F. Stancu, Tetraquarks with heavy flavors, Phys. Rev. D **57**, 6778 (1998).

TABLE XIII: The average contributions of each part of the Hamiltonian to the $1D$ -wave $T_{(ccc\bar{c})}$ configurations. $\langle T \rangle$ stands for the contribution of the kinetic energy term. $\langle V^{Lin} \rangle$ and $\langle V^{Coul} \rangle$ stand for the contributions from the linear confinement potential and Coulomb type potential, respectively. $\langle V^{SS} \rangle$, $\langle V^T \rangle$, and $\langle V^{LS} \rangle$ stand for the contributions from the spin-spin interaction term, the tensor potential term, and the spin-orbit interaction term, respectively.

J^{PC}	Configuration	Mass	$\langle T \rangle$	$\langle V^{Lin} \rangle$	$\langle V^{Coul} \rangle$	$\langle V^{SS} \rangle$	$\langle V^T \rangle$	$\langle V^{LS} \rangle$	
0^{+-}	$1^3P_{0^{+-}(\bar{66})_c(\xi_1\xi_3,\xi_2\xi_3)}$	6868	732	837	-636	6.18	0	-2.28	
	$1^3P_{0^{+-}(\bar{33})_c(\xi_1\xi_3,\xi_2\xi_3)}$	6948	749	876	-601	-2.66	0	-4.73	
	$1^5D_{0^{+-}(\bar{33})_c(\xi_1,\xi_2)}$	7054	809	924	-572	9.25	-5.91	-43.52	
0^{++}	$1^1S_{0^{++}(\bar{33})_c(\xi_1\xi_2)}$	6838	769	818	-657	-24.14	0	0	
	$1^1S_{0^{++}(\bar{66})_c(\xi_1\xi_2)}$	6957	788	877	-603	-37.55	0	0	
	$1^3P_{0^{++}(\bar{66})_c(\xi_1\xi_3,\xi_2\xi_3)}$	6857	745	830	-642	-2.02	-2.35	-2.35	
	$1^3P_{0^{++}(\bar{33})_c(\xi_1\xi_3,\xi_2\xi_3)}$	6944	754	873	-603	-6.08	-0.96	-4.79	
	$1^3P_{0^{++}(\bar{66})_c(\xi_1\xi_2)}$	7053	775	925	-553	-15.43	2.49	-12.47	
	$1^5D_{0^{++}(\bar{33})_c(\xi_1,\xi_2)}$	7051	798	927	-577	9.84	-4.46	-35.39	
	$1^5D_{0^{++}(\bar{33})_c(\xi_3)}$	6968	783	883	-603	10.84	-4.59	-32.12	
	$1^5D_{0^{++}(\bar{66})_c(\xi_1\xi_2)}$	7013	802	902	-585	9.78	-5.96	-41.73	
	$1^3S_{1^{+-}(\bar{66})_c(\xi_1\xi_3,\xi_2\xi_3)}$	7002	739	908	-584	7.19	0	0	
	$1^3S_{1^{+-}(\bar{33})_c(\xi_1\xi_3,\xi_2\xi_3)}$	7007	743	906	-571	-2.36	0	0	
1^{+-}	$1^3S_{1^{+-}(\bar{66})_c(\xi_1\xi_2)}$	6973	768	888	-595	-20.14	0	0	
	$1^1P_{1^{+-}(\bar{33})_c(\xi_1\xi_2)}$	6871	767	834	-637	-23.89	0	0	
	$1^1P_{1^{+-}(\bar{66})_c(\xi_1\xi_2)}$	7052	776	924	-554	-26.86	0	0	
	$1^3P_{1^{+-}(\bar{66})_c(\xi_1\xi_3,\xi_2\xi_3)}$	6867	733	836	-637	6.2	-0.86	-2.58	
	$1^3P_{1^{+-}(\bar{33})_c(\xi_1\xi_3,\xi_2\xi_3)}$	6946	753	874	-603	-2.68	-1.79	-5.37	
	$1^5P_{1^{+-}(\bar{66})_c(\xi_1\xi_2)}$	7069	754	937	-545	7.04	0.6	-16.07	
	$1^3D_{1^{+-}(\bar{33})_c(\xi_1,\xi_2)}$	7062	781	937	-570	-1.23	-0.13	-17.01	
	$1^3D_{1^{+-}(\bar{33})_c(\xi_3)}$	6978	767	891	-597	-1.51	1.23	-15.46	
	$1^3D_{1^{+-}(\bar{66})_c(\xi_1\xi_3,\xi_2\xi_3)}$	7092	782	953	-555	1.73	-0.06	-19.86	
	$1^3D_{1^{+-}(\bar{33})_c(\xi_1\xi_3,\xi_2\xi_3)}$	7026	786	912	-575	-4.9	-2.18	-21.88	
	$1^3D_{1^{+-}(\bar{66})_c(\xi_1\xi_2)}$	7008	804	901	-586	-18.28	-2.98	-20.89	
	$1^5D_{1^{+-}(\bar{33})_c(\xi_1,\xi_2)}$	7064	794	933	-566	8.98	-2.86	-35.06	
	1^{++}	$1^3S_{1^{++}(\bar{66})_c(\xi_1\xi_3,\xi_2\xi_3)}$	6991	747	903	-588	-3.32	0	0
		$1^3S_{1^{++}(\bar{33})_c(\xi_1\xi_3,\xi_2\xi_3)}$	7003	746	903	-572	-6.56	0	0
$1^3P_{1^{++}(\bar{66})_c(\xi_1\xi_3,\xi_2\xi_3)}$		6861	739	833	-640	-2	2.03	-2.61	
$1^3P_{1^{++}(\bar{33})_c(\xi_1\xi_3,\xi_2\xi_3)}$		6944	755	873	-603	-6.09	-0.6	-5.39	
$1^3P_{1^{++}(\bar{66})_c(\xi_1\xi_2)}$		7051	779	923	-555	-15.54	-3.14	-9.43	
$1^3D_{1^{++}(\bar{33})_c(\xi_1,\xi_2)}$		7070	783	939	-562	-0.47	-0.76	-20.53	
$1^3D_{1^{++}(\bar{66})_c(\xi_1\xi_3,\xi_2\xi_3)}$		7096	777	956	-554	2.85	1.81	-19.64	
$1^3D_{1^{++}(\bar{33})_c(\xi_1\xi_3,\xi_2\xi_3)}$		7028	784	913	-574	-4.41	-1.4	-21.78	
$1^5D_{1^{++}(\bar{33})_c(\xi_1,\xi_2)}$		7059	786	934	-572	9.62	-2.17	-28.72	
$1^5D_{1^{++}(\bar{33})_c(\xi_3)}$		6976	772	889	-599	10.6	-2.24	-26.09	
$1^5D_{1^{++}(\bar{66})_c(\xi_1\xi_2)}$	7022	787	911	-580	9.49	-2.88	-33.63		
2^{+-}	$1^3P_{2^{+-}(\bar{66})_c(\xi_1\xi_3,\xi_2\xi_3)}$	6873	725	841	-633	6.1	0.17	2.53	
	$1^3P_{2^{+-}(\bar{33})_c(\xi_1\xi_3,\xi_2\xi_3)}$	6959	735	884	-595	-2.57	0.34	5.15	
	$1^5P_{2^{+-}(\bar{66})_c(\xi_1\xi_2)}$	7072	751	939	-544	6.99	-4.13	-8.86	
	$1^1D_{2^{+-}(\bar{66})_c(\xi_1,\xi_2)}$	6985	727	895	-575	5.62	0	0	
	$1^1D_{2^{+-}(\bar{33})_c(\xi_1,\xi_2)}$	7087	760	953	-553	-4.84	0	0	
	$1^3D_{2^{+-}(\bar{33})_c(\xi_1,\xi_2)}$	7073	765	947	-564	-1.19	0.12	-5.47	
	$1^3D_{2^{+-}(\bar{33})_c(\xi_3)}$	6985	755	898	-592	-1.48	-1.2	-5.02	
	$1^3D_{2^{+-}(\bar{66})_c(\xi_1\xi_3,\xi_2\xi_3)}$	7106	763	964	-549	1.67	0.06	-6.35	
	$1^3D_{2^{+-}(\bar{33})_c(\xi_1\xi_3,\xi_2\xi_3)}$	7045	760	927	-565	-4.63	2.05	-6.87	
	$1^3D_{2^{+-}(\bar{66})_c(\xi_1\xi_2)}$	7028	774	917	-575	-17.3	2.8	-6.53	
	$1^5D_{2^{+-}(\bar{33})_c(\xi_1,\xi_2)}$	7082	768	948	-556	8.53	1.16	-19.86	

TABLE XIV: The average contributions of each part of the Hamiltonian to the $1D$ -wave $T_{(ccc\bar{c})}$ configurations (Continued).

J^{PC}	Configuration	Mass	$\langle T \rangle$	$\langle V^{Lin} \rangle$	$\langle V^{Coul} \rangle$	$\langle V^{SS} \rangle$	$\langle V^T \rangle$	$\langle V^{LS} \rangle$
	$1^3S_{2^{++}(66)_c(\xi_1\xi_2)}$	7004	731	911	-581	11.30	0	0
	$1^3P_{2^{++}(66)_c(\xi_1\xi_2\xi_3)}$	6864	735	835	-638	-1.99	-0.4	2.58
	$1^3P_{2^{++}(33)_c(\xi_1\xi_2\xi_3)}$	6955	739	882	-597	-5.89	0.12	5.19
	$1^3P_{2^{++}(66)_c(\xi_1\xi_2)}$	7073	748	941	-543	-14.59	0.59	8.79
	$1^1D_{2^{++}(66)_c(\xi_1\xi_2)}$	6955	733	883	-598	5.68	0	0
	$1^1D_{2^{++}(33)_c(\xi_1\xi_2)}$	7073	764	947	-563	-6.38	0	0
	$1^1D_{2^{++}(66)_c(\xi_3)}$	6964	744	894	-613	6.43	0	0
2^{++}	$1^1D_{2^{++}(33)_c(\xi_3)}$	6986	754	899	-591	-7.33	0	0
	$1^1D_{2^{++}(33)_c(\xi_1\xi_2)}$	6859	769	829	-647	-24.01	0	0
	$1^1D_{2^{++}(66)_c(\xi_1\xi_2)}$	7018	787	910	-579	-31.28	0	0
	$1^3D_{2^{++}(33)_c(\xi_1\xi_2)}$	7085	762	952	-554	-0.44	0.72	-6.52
	$1^3D_{2^{++}(66)_c(\xi_1\xi_2\xi_3)}$	7105	764	963	-549	2.77	-1.76	-6.36
	$1^3D_{2^{++}(33)_c(\xi_1\xi_2\xi_3)}$	7045	760	927	-565	-4.2	1.33	-6.87
	$1^5D_{2^{++}(33)_c(\xi_1\xi_2)}$	7073	766	946	-564	9.24	0.89	-16.46
	$1^5D_{2^{++}(33)_c(\xi_3)}$	6989	752	900	-591	10.19	0.92	-14.97
	$1^5D_{2^{++}(66)_c(\xi_1\xi_2)}$	7040	761	925	-570	9.03	1.17	-19.07
	$1^5P_{3^{+-}(66)_c(\xi_1\xi_2)}$	7102	711	964	-529	6.38	1.08	16.13
	$1^3D_{3^{+-}(33)_c(\xi_1\xi_2)}$	7089	743	960	-555	-1.14	-0.03	10.41
	$1^3D_{3^{+-}(33)_c(\xi_3)}$	7002	733	911	-583	-1.43	0.32	9.54
3^{+-}	$1^3D_{3^{+-}(66)_c(\xi_1\xi_2\xi_3)}$	7124	739	979	-539	1.6	-0.02	12.01
	$1^3D_{3^{+-}(33)_c(\xi_1\xi_2\xi_3)}$	7062	736	942	-555	-4.4	-0.55	13
	$1^3D_{3^{+-}(66)_c(\xi_1\xi_2)}$	7043	752	930	-566	-16.57	-0.76	12.43
	$1^5D_{3^{+-}(33)_c(\xi_1\xi_2)}$	7103	740	965	-545	8.04	2.89	0
	$1^3D_{3^{++}(33)_c(\xi_1\xi_2)}$	7103	738	967	-545	-0.4	-0.2	12.34
	$1^3D_{3^{++}(66)_c(\xi_1\xi_2\xi_3)}$	7126	736	981	-538	2.59	0.47	11.94
3^{++}	$1^3D_{3^{++}(33)_c(\xi_1\xi_2\xi_3)}$	7063	735	942	-555	-3.99	-0.36	12.97
	$1^5D_{3^{++}(33)_c(\xi_1\xi_2)}$	7091	742	961	-555	8.81	2.24	0
	$1^5D_{3^{++}(33)_c(\xi_3)}$	7005	730	913	-582	9.74	2.32	0
	$1^5D_{3^{++}(66)_c(\xi_1\xi_2)}$	7060	734	942	-559	8.52	2.92	0
4^{+-}	$1^5D_{4^{+-}(33)_c(\xi_1\xi_2)}$	7122	715	982	-536	7.62	-1.36	23.36
	$1^5D_{4^{++}(33)_c(\xi_1\xi_2)}$	7108	720	975	-546	8.42	-1.07	19.74
4^{++}	$1^5D_{4^{++}(33)_c(\xi_3)}$	7020	710	925	-573	9.34	-1.11	18.09
	$1^5D_{4^{++}(66)_c(\xi_1\xi_2)}$	7079	710	957	-549	8.09	-1.38	22.5

TABLE XV: The average contributions of each part of the Hamiltonian to the 1D-wave $T_{(bb\bar{b}\bar{b})}$ configurations.

J^{PC}	Configuration	Mass	$\langle T \rangle$	$\langle V^{Lin} \rangle$	$\langle V^{Coul} \rangle$	$\langle V^{SS} \rangle$	$\langle V^T \rangle$	$\langle V^{LS} \rangle$
0^{+-}	$1^3P_{0^{+-}(6\bar{6})_c(\xi_1\xi_3,\xi_2\xi_3)}$	19693	677	482	-876	2.6	0	-0.91
	$1^3P_{0^{+-}(3\bar{3})_c(\xi_1\xi_3,\xi_2\xi_3)}$	19775	667	514	-812	-0.98	0	-1.77
	$1^5D_{0^{+-}(3\bar{3})_c(\xi_1,\xi_2)}$	19884	674	561	-746	3.24	-1.98	-14.56
0^{++}	$1^1S_{0^{++}(3\bar{3})_c(\xi_1\xi_2)}$	19677	697	475	-893	-9.68	0	0
	$1^1S_{0^{++}(6\bar{6})_c(\xi_1\xi_2)}$	19796	681	523	-801	-13.94	0	0
	$1^3P_{0^{++}(6\bar{6})_c(\xi_1\xi_3,\xi_2\xi_3)}$	19688	684	480	-881	-0.91	-0.92	-0.92
	$1^3P_{0^{++}(3\bar{3})_c(\xi_1\xi_3,\xi_2\xi_3)}$	19773	670	513	-813	-2.37	-0.36	-1.78
	$1^3P_{0^{++}(6\bar{6})_c(\xi_1,\xi_2)}$	19884	655	557	-728	-5.53	0.86	-4.3
	$1^5D_{0^{++}(3\bar{3})_c(\xi_1,\xi_2)}$	19873	674	559	-757	3.56	-1.53	-12.13
	$1^5D_{0^{++}(3\bar{3})_c(\xi_3)}$	19800	678	525	-803	4.05	-1.64	-11.46
	$1^5D_{0^{++}(6\bar{6})_c(\xi_1\xi_2)}$	19847	676	544	-768	3.49	-2.04	-14.25
	1^{+-}	$1^3S_{1^{+-}(6\bar{6})_c(\xi_1\xi_3,\xi_2\xi_3)}$	19812	662	535	-796	2.97	0
$1^3S_{1^{+-}(3\bar{3})_c(\xi_1\xi_3,\xi_2\xi_3)}$		19828	653	536	-768	-0.73	0	0
$1^3S_{1^{+-}(6\bar{6})_c(\xi_1,\xi_2)}$		19802	671	526	-796	-7.59	0	0
$1^1P_{1^{+-}(3\bar{3})_c(\xi_1\xi_2)}$		19711	689	488	-864	-9.56	0	0
$1^1P_{1^{+-}(6\bar{6})_c(\xi_1,\xi_2)}$		19883	656	557	-728	-9.59	0	0
$1^3P_{1^{+-}(6\bar{6})_c(\xi_1\xi_3,\xi_2\xi_3)}$		19692	678	482	-877	2.61	-0.34	-1.02
$1^3P_{1^{+-}(3\bar{3})_c(\xi_1\xi_3,\xi_2\xi_3)}$		19774	669	514	-813	-0.98	-0.67	-2
$1^5P_{1^{+-}(6\bar{6})_c(\xi_1,\xi_2)}$		19890	646	561	-722	2.51	0.21	-5.67
$1^3D_{1^{+-}(3\bar{3})_c(\xi_1,\xi_2)}$		19877	667	562	-753	-0.44	-0.04	-5.96
$1^3D_{1^{+-}(3\bar{3})_c(\xi_3)}$		19803	672	528	-799	-0.63	0.45	-5.64
$1^3D_{1^{+-}(6\bar{6})_c(\xi_1\xi_3,\xi_2\xi_3)}$		19906	662	573	-731	0.66	-0.02	-6.86
$1^3D_{1^{+-}(3\bar{3})_c(\xi_1\xi_3,\xi_2\xi_3)}$		19856	668	548	-758	-1.73	-0.75	-7.58
$1^3D_{1^{+-}(6\bar{6})_c(\xi_1,\xi_2)}$		19845	678	543	-769	-6.61	-1.02	-7.15
$1^5D_{1^{+-}(3\bar{3})_c(\xi_1,\xi_2)}$		19887	668	563	-742	3.2	-0.97	-11.95
1^{++}		$1^3S_{1^{++}(6\bar{6})_c(\xi_1\xi_3,\xi_2\xi_3)}$	19807	667	533	-799	-1.48	0
	$1^3S_{1^{++}(3\bar{3})_c(\xi_1\xi_3,\xi_2\xi_3)}$	19827	655	535	-770	-2.46	0	0
	$1^3P_{1^{++}(6\bar{6})_c(\xi_1\xi_3,\xi_2\xi_3)}$	19690	681	481	-879	-0.91	0.8	-1.03
	$1^3P_{1^{++}(3\bar{3})_c(\xi_1\xi_3,\xi_2\xi_3)}$	19773	670	513	-813	-2.37	-0.22	-2.01
	$1^3P_{1^{++}(6\bar{6})_c(\xi_1,\xi_2)}$	19883	657	556	-728	-5.55	-1.08	-3.24
	$1^3D_{1^{++}(3\bar{3})_c(\xi_1,\xi_2)}$	19889	664	565	-740	-0.13	-0.26	-7.1
	$1^3D_{1^{++}(6\bar{6})_c(\xi_1\xi_3,\xi_2\xi_3)}$	19907	660	574	-730	0.97	0.63	-6.83
	$1^3D_{1^{++}(3\bar{3})_c(\xi_1\xi_3,\xi_2\xi_3)}$	19856	667	548	-757	-1.6	-0.49	-7.57
	$1^5D_{1^{++}(3\bar{3})_c(\xi_1,\xi_2)}$	19876	669	561	-754	3.52	-0.75	-9.98
	$1^5D_{1^{++}(3\bar{3})_c(\xi_3)}$	19802	673	527	-800	4.01	-0.81	-9.44
$1^5D_{1^{++}(6\bar{6})_c(\xi_1\xi_2)}$	19850	670	546	-765	3.44	-1	-11.69	
2^{+-}	$1^3P_{2^{+-}(6\bar{6})_c(\xi_1\xi_3,\xi_2\xi_3)}$	19695	674	483	-874	2.58	0.07	1.01
	$1^3P_{2^{+-}(3\bar{3})_c(\xi_1\xi_3,\xi_2\xi_3)}$	19779	660	517	-807	-0.96	0.13	1.96
	$1^5P_{2^{+-}(6\bar{6})_c(\xi_1,\xi_2)}$	19891	645	561	-721	2.5	-1.46	-3.14
	$1^1D_{2^{+-}(6\bar{6})_c(\xi_1,\xi_2)}$	19807	648	525	-777	2.21	0	0
	$1^1D_{2^{+-}(3\bar{3})_c(\xi_1,\xi_2)}$	19895	654	569	-734	-1.73	0	0
	$1^3D_{2^{+-}(3\bar{3})_c(\xi_1,\xi_2)}$	19881	660	564	-749	-0.43	0.04	-1.95
	$1^3D_{2^{+-}(3\bar{3})_c(\xi_3)}$	19806	667	529	-796	-0.62	-0.44	-1.86
	$1^3D_{2^{+-}(6\bar{6})_c(\xi_1\xi_3,\xi_2\xi_3)}$	19910	654	576	-727	0.65	0.02	-2.24
	$1^3D_{2^{+-}(3\bar{3})_c(\xi_1\xi_3,\xi_2\xi_3)}$	19863	657	552	-751	-1.69	0.73	-2.46
	$1^3D_{2^{+-}(6\bar{6})_c(\xi_1,\xi_2)}$	19852	666	548	-763	-6.44	0.99	-2.31
	$1^5D_{2^{+-}(3\bar{3})_c(\xi_1,\xi_2)}$	19893	657	567	-736	3.12	0.41	-6.98

TABLE XVI: The average contributions of each part of the Hamiltonian to the $1D$ -wave $T_{(bb\bar{b}\bar{b})}$ configurations (Continued).

J^{PC}	Configuration	Mass	$\langle T \rangle$	$\langle V^{Lin} \rangle$	$\langle V^{Coul} \rangle$	$\langle V^{SS} \rangle$	$\langle V^T \rangle$	$\langle V^{LS} \rangle$
	$1^3S_{2^{++}(66)_c(\xi_1\xi_2)}$	19814	653	534	-785	4.39	0	0
	$1^3P_{2^{++}(66)_c(\xi_1\xi_3,\xi_2\xi_3)}$	19691	679	481	-878	-0.9	-0.16	1.03
	$1^3P_{2^{++}(33)_c(\xi_1\xi_3,\xi_2\xi_3)}$	19777	662	516	-809	-2.33	0.04	1.97
	$1^3P_{2^{++}(66)_c(\xi_1\xi_2)}$	19891	644	562	-721	-5.38	0.21	3.13
	$1^1D_{2^{++}(66)_c(\xi_1,\xi_2)}$	19773	661	515	-814	2.27	0	0
	$1^1D_{2^{++}(33)_c(\xi_1,\xi_2)}$	19881	660	564	-749	-2.37	0	0
	$1^1D_{2^{++}(66)_c(\xi_3)}$	19770	674	521	-835	2.53	0	0
2^{++}	$1^1D_{2^{++}(33)_c(\xi_3)}$	19806	666	530	-796	-2.9	0	0
	$1^1D_{2^{++}(33)_c(\xi_1,\xi_2)}$	19697	695	484	-880	-9.67	0	0
	$1^1D_{2^{++}(66)_c(\xi_1,\xi_2)}$	19848	672	546	-766	-11.5	0	0
	$1^3D_{2^{++}(33)_c(\xi_1,\xi_2)}$	19894	655	568	-735	-0.12	0.26	-2.31
	$1^3D_{2^{++}(66)_c(\xi_1,\xi_3,\xi_2\xi_3)}$	19910	654	576	-727	0.96	-0.62	-2.24
	$1^3D_{2^{++}(33)_c(\xi_1,\xi_3,\xi_2\xi_3)}$	19862	657	552	-751	-1.56	0.47	-2.46
	$1^5D_{2^{++}(33)_c(\xi_1,\xi_2)}$	19881	660	564	-749	3.45	0.32	-5.86
	$1^5D_{2^{++}(33)_c(\xi_3)}$	19807	665	530	-795	3.93	0.34	-5.54
	$1^5D_{2^{++}(66)_c(\xi_1,\xi_2)}$	19856	659	550	-759	3.36	0.42	-6.83
	$1^5P_{3^{+-}(66)_c(\xi_1,\xi_2)}$	19902	627	569	-711	2.39	0.4	5.98
	$1^3D_{3^{+-}(33)_c(\xi_1,\xi_2)}$	19887	651	568	-744	-0.42	-0.01	3.81
	$1^3D_{3^{+-}(33)_c(\xi_3)}$	19812	657	533	-789	-0.61	0.12	3.62
3^{+-}	$1^3D_{3^{+-}(66)_c(\xi_1\xi_3,\xi_2\xi_3)}$	19917	643	581	-720	0.64	-0.01	4.36
	$1^3D_{3^{+-}(33)_c(\xi_1\xi_3,\xi_2\xi_3)}$	19869	647	557	-745	-1.64	-0.2	4.78
	$1^3D_{3^{+-}(66)_c(\xi_1,\xi_2)}$	19857	657	552	-757	-6.3	-0.28	4.52
	$1^5D_{3^{+-}(33)_c(\xi_1,\xi_2)}$	19901	645	573	-729	3.03	1.05	0
	$1^3D_{3^{++}(33)_c(\xi_1,\xi_2)}$	19901	644	573	-729	-0.12	-0.07	4.5
	$1^3D_{3^{++}(66)_c(\xi_1\xi_3,\xi_2\xi_3)}$	19917	642	581	-720	0.93	0.17	4.35
3^{++}	$1^3D_{3^{++}(33)_c(\xi_1\xi_3,\xi_2\xi_3)}$	19869	646	557	-745	-1.52	-0.13	4.78
	$1^5D_{3^{++}(33)_c(\xi_1,\xi_2)}$	19887	650	569	-743	3.37	0.82	0
	$1^5D_{3^{++}(33)_c(\xi_3)}$	19813	655	534	-788	3.83	0.88	0
	$1^5D_{3^{++}(66)_c(\xi_1,\xi_2)}$	19864	647	555	-751	3.26	1.08	0
4^{+-}	$1^5D_{4^{+-}(33)_c(\xi_1,\xi_2)}$	19908	634	578	-722	2.94	-0.51	8.74
	$1^5D_{4^{++}(33)_c(\xi_1,\xi_2)}$	19894	640	573	-737	3.29	-0.4	7.41
4^{++}	$1^5D_{4^{++}(33)_c(\xi_3)}$	19819	645	538	-782	3.75	-0.43	7.02
	$1^5D_{4^{++}(66)_c(\xi_1,\xi_2)}$	19871	636	560	-744	3.17	-0.52	8.56

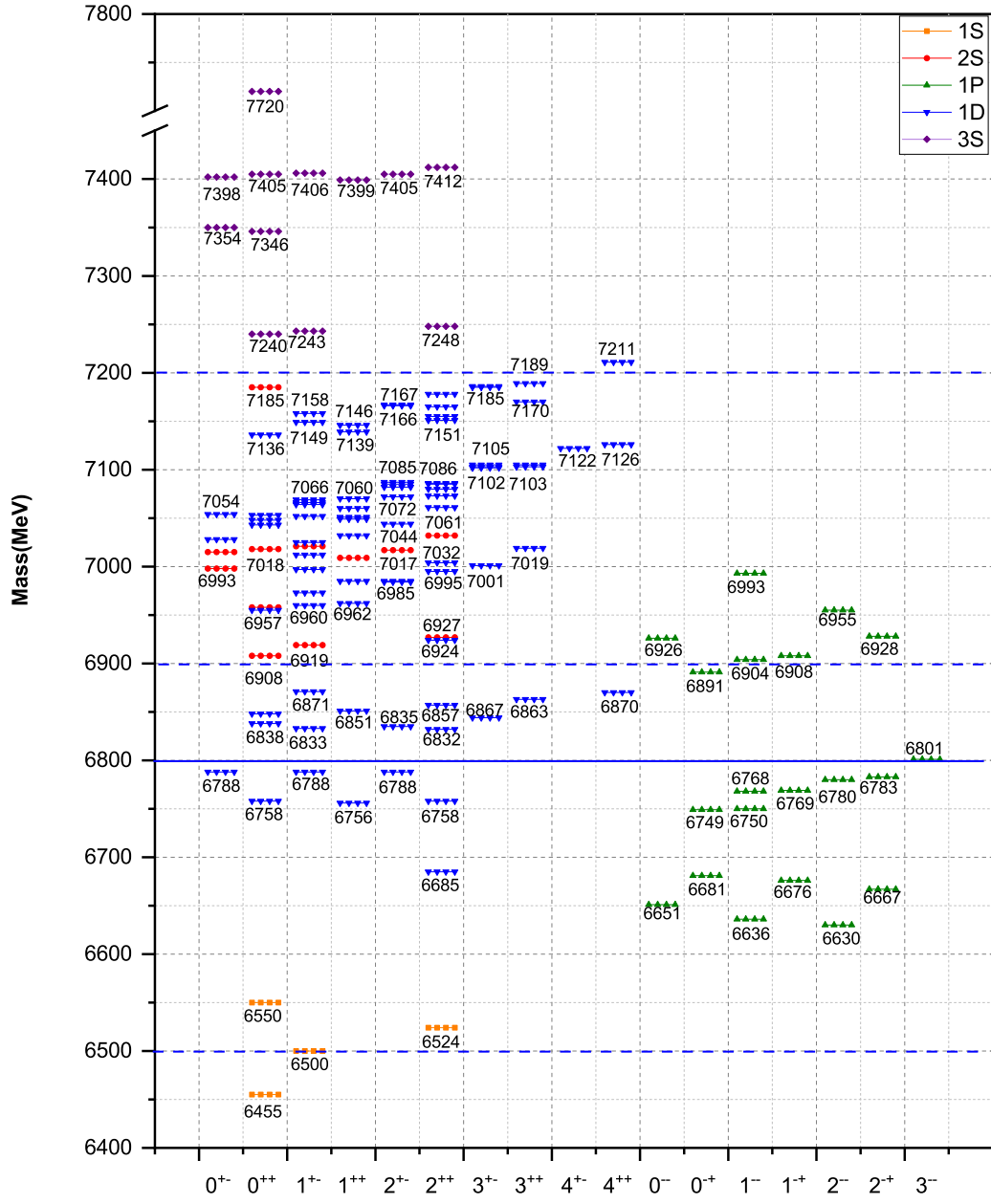


FIG. 2: $T_{(ccc)}$ mass spectrum up to the second radial excitations.

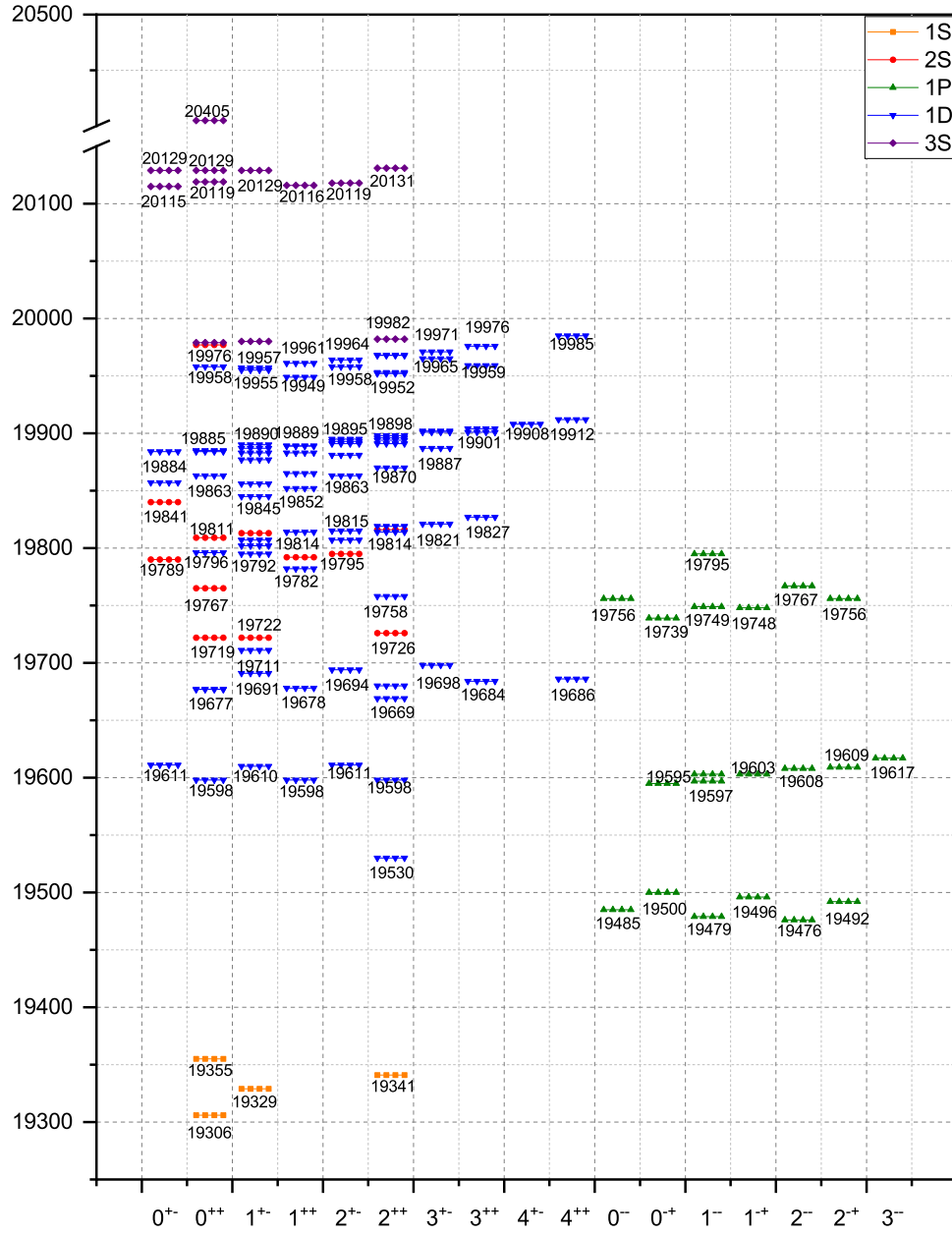


FIG. 3: $T_{(bbbb)}$ mass spectrum up to the second radial excitations.